S E P A R A T A

Revista Geológica de Chile 35 (1): 79-104. January, 2008

Revista Geológica de Chile

New time-constraints on provenance, metamorphism and exhumation of the Bahía Mansa Metamorphic Complex on the Main Chiloé Island, south-central Chile

Paul Duhart[1], Alberto C. Adriasola[2]

[1] *Servicio Nacional de Geología y Minería, Oficina Técnica Puerto Varas, Casilla 613, Puerto Varas, Chile.*
pduhart@sernageomin.cl
[2] *Fugro-Robertson Limited, Llandudno LL30 1SA, United Kingdom.*
aam@fugro-robertson.com

ISSN 0716-0208
Editada por el Servicio Nacional de Geología y Minería
con la colaboración científica de la Sociedad Geológica de Chile
Avda. Santa María 0104, Casilla 10465, Santiago, Chile.
revgeologica@sernageomin.cl; http://www.scielo.cl/rgch.htm; http://www.sernageomin.cl

Revista Geológica de Chile 35 (1): 79-104. January, 2008

Revista Geológica de Chile

www.scielo.cl/rgch.htm

New time-constraints on provenance, metamorphism and exhumation of the Bahía Mansa Metamorphic Complex on the Main Chiloé Island, south-central Chile

Paul Duhart[1], Alberto C. Adriasola[2]

[1] *Servicio Nacional de Geología y Minería, Oficina Técnica Puerto Varas, Casilla 613, Puerto Varas, Chile. pduhart@sernageomin.cl*

[2] *Fugro-Robertson Limited, Llandudno LL30 1SA, United Kingdom. aam@fugro-robertson.com*

ABSTRACT. The Coastal Ranges in the western part of the Chiloé Archipelago represent an emerged forearc high at the subduction front of south-central Chile. Prior to the Cenozoic framework of the subducting Farallon and Nazca plates beneath the South American plate, the history of the metamorphic basement in the Coastal Ranges involves episodes of subduction and/or accretion of oceanic and ensialic material along the proto-Pacific margin of Gondwana. Along different segments of the Main Chiloé Island the thermal record of the metamorphic basement rocks includes regional metamorphism, exhumation and finally magmatism. Detrital zircons conventional U-Pb ages from a pelitic schist of the Central Segment of the Main Chiloé Island constrain the maximum possible sedimentation age to the Carboniferous (310 Ma). Other concordant zircon fractions (360, 390 and 412 Ma) suggest Ordovician primary sources. The sedimentary provenance of zircons could correspond to continental magmatic rocks of similar ages presently exposed in adjacent areas such as Nahuelbuta Mountains and Principal Cordillera and, additionally, from distal areas in the North-Patagonian and Deseado massifs. Widespread metamorphism in greenschist facies is well represented in the basement unit of the Main Chiloé Island. K-Ar and $^{40}Ar/^{39}Ar$ cooling ages in white mica range between 245 to 220 Ma, interpreted as near the peak of metamorphism during Middle to early Late Triassic times. Zircon and apatite fission-track (FT) central ages in metamorphic rocks range from Late Jurassic (*ca*. 156 Ma) to Eocene (*ca*. 38 Ma) and are accompanied by relatively large dispersions. The modelling of the zircon FT single-grain age distributions depicts younger deconvoluted Late Cretaceous peak (*ca*. 80 Ma) and the apatite modelling shows two populations, an older Late Cretaceous peak (*ca*. 64-91 Ma) and a younger Eocene peak (*ca*. 38-53 Ma). The zircon and apatite Late Cretaceous peaks together with the presence of a marine sedimentary succession of presumably later Late Cretaceous age found at the forearc slope of the Main Chiloé Island, suggest exhumation of the metamorphic unit during the early Late Cretaceous. Magmatic zircons from a granodioritic body (Metalqui Pluton) emplaced in pelitic schists within the Central Segment of the Main Chiloé Island, a differentially uplifted block in relation to the northern and southern segments, gave an Eocene U-Pb crystallization age (39.6±0.3 Ma). Upper Eocene (*ca*. 37 Ma) biotite-bearing porphyric dacitic sills and dikes (Gamboa Dacite) also occur within the Central Segment. Zircon and apatite FT concordant ages (*ca*. 36 Ma) indicated rapid cooling for these subvolcanic rocks during Eocene times. According to this data, Eocene apatite central and modelling single-grain FT ages detected in the metamorphic rocks probably represent thermal resetting by shallow magmatism, coeval with the Gamboa Dacite and possibly the Metalqui Pluton.

Keywords: Metamorphic/post-metamorphic thermochronology, Chilean forearc, Cenozoic magmatism, South-Central Andes.

RESUMEN. **Nuevas restricciones temporales sobre proveniencia, metamorfismo y exhumación del Complejo Metamórfico Bahía Mansa en la Isla Grande de Chiloé, centro-sur de Chile.** La Cordillera de la Costa, en la parte occidental del Archipiélago de Chiloé, representa un alto emergido de antearco en el frente de subducción del centro-sur de Chile. Previo al Cenozoico, período en el cual la región ha sido dominada por un sistema de subducción de la placas Farallón y Nazca por debajo de la placa Sudamericana, la historia del basamento metamórfico de la Cordillera de la Costa involucró episodios de subducción y/o acreción de material oceánico y ensiálico a lo largo del margen proto-Pacífico de Gondwana. El registro termal del basamento metamórfico incluye metamorfismo regional, exhumación y finalmente magmatismo para los distintos segmentos de la Isla Grande de Chiloé. Edades convencionales U-Pb en circones detríticos de un esquisto pelítico del Segmento Central de la Isla Grande de Chiloé, restringen la posible edad máxima de sedimentación al Carbonífero (310 Ma). Otras fracciones de circones concordantes (360, 390 y 412 Ma) sugieren fuentes primarias del Ordovícico. La proveniencia sedimentaria de los circones podría corresponder a rocas magmáticas continentales de edades similares actualmente expuestas en áreas adyacentes, tales como en las cordilleras de Nahuelbuta y Principal y, adicionalmente, desde áreas distales en los macizos Nor-Patagónico y Deseado. Un extenso metamorfismo en la facies de esquistos verdes está bien representado en las rocas del basamento metamórfico. Edades de enfriamiento K-Ar y $^{40}Ar/^{39}Ar$ en mica blanca se sitúan en el rango de entre 245 y 220 Ma, y son interpretadas como cercanas al máximo metamórfico ocurrido durante el Triásico Medio-Triásico Tardío temprano. Edades centrales por medio de trazas de fisión (TF) en circón y apatita se sitúan en el rango Jurásico Tardío (*ca*. 156 Ma) al Eoceno (*ca*. 38 Ma) y están acompañadas por una relativa gran dispersión. El modelamiento de las distribuciones de las TF en un grano único de circón, muestra un máximo en el Cretácico Tardío (*ca*. 80 Ma) y, el modelamiento en apatita, muestra dos poblaciones, una antigua con un máximo en el Cretácico Tardío (*ca*. 64-91 Ma), y una joven, con un máximo en el Eoceno (*ca*. 38-53 Ma). Los máximos de circón y apatita en el Cretácico Tardío, junto con la presencia de abundantes sedimentos de presumible edad cretácica tardía alta, que se encuentran en la cuenca de antearco, al oeste de la Isla Grande de Chiloé, sugieren que la exhumación de la unidad metamórfica ocurrió durante el Cretácico Tardío temprano. Circones magmáticos de un cuerpo granodiorítico (Plutón Metalqui) emplazado en esquistos pelíticos dentro del Segmento Central de la Isla Grande de Chiloé, un bloque diferencialmente alzado en relación a los segmentos norte-sur, dieron una edad de cristalización U-Pb eocena de 39,6±0,3 Ma. Diques y 'sills' dacíticos que contienen biotita (Dacita Gamboa) del Eoceno Superior (*ca*. 37 Ma) también ocurren dentro del Segmento Central. Edades concordantes de TF en circón y apatita (*ca*. 36 Ma) indican un rápido enfriamiento de las rocas subvolcánicas durante el Eoceno. De acuerdo con estos datos, las edades centrales y modeladas de TF en apatita del Eoceno, detectadas en rocas metamórficas, probablemente representen un reajuste termal debido a magmatismo poco profundo, contemporáneo con la Dacita Gamboa y, posiblemente, con el Plutón Metalqui.

Palabras claves: Termocronología metamórfica/post-metamórfica, Antearco chileno, Magmatismo Cenozoico, Andes del Centro-sur.

1. Introduction

The western portion of the Chiloé Archipelago forms part of the Coastal Ranges of south-central Chile between 41°45' and 43°30'S (Fig. 1). Its morphology is characterized by relatively low altitudes and sea-flooded coastlines. The oldest rocks of the Chiloé Archipelago have been traditionally interpreted as remnants of a Paleozoic subduction complex whose sedimentary provenance remains largely unknown. Progressive mapping campaigns supported by geochronological studies have led to the correlation of these rocks to the Bahía Mansa Metamorphic Complex (Duhart *et al.*, 2000, 2001), which is well exposed along the Coastal Ranges between 39° and ~41°30'S. An extensive set of data of U-Pb, K-Ar, and $^{40}Ar/^{39}Ar$ ages for this latter unit indicates that the greenschist facies metamorphism evolved during Permian-Triassic times (*ca*. 260-220 Ma; Duhart *et al*., 2001).

On Chiloé Archipelago, the metamorphic basement is partly covered by Cenozoic marine and continental sedimentary rocks, Cenozoic volcanic rocks, and Pleistocene glacial and glaciofluvial deposits (Fig. 2). Recent mapping and conventional U-Pb dating (Arenas and Duhart, 2003) have identified for the first time an Eocene pluton in the northern part of the archipelago (Fig. 2). The Main Chiloé Island of the Chiloé Archipelago has been subdivided into three segments along NW-trending lineaments, mainly based on aeromagnetic anomalies and morphology (Fig. 2; Muñoz *et al.*, 1999). The Northern and Southern segments of the island (herein defined as NSIC and SSIC, respectively) correspond to areas with low relief and elevations of ~350 m above sea level, whereas the Central Segment (herein defined as CSIC), which includes the so-called Piuchén Cordillera, displays a more rugged topography and summits at ~800 m above sea level.

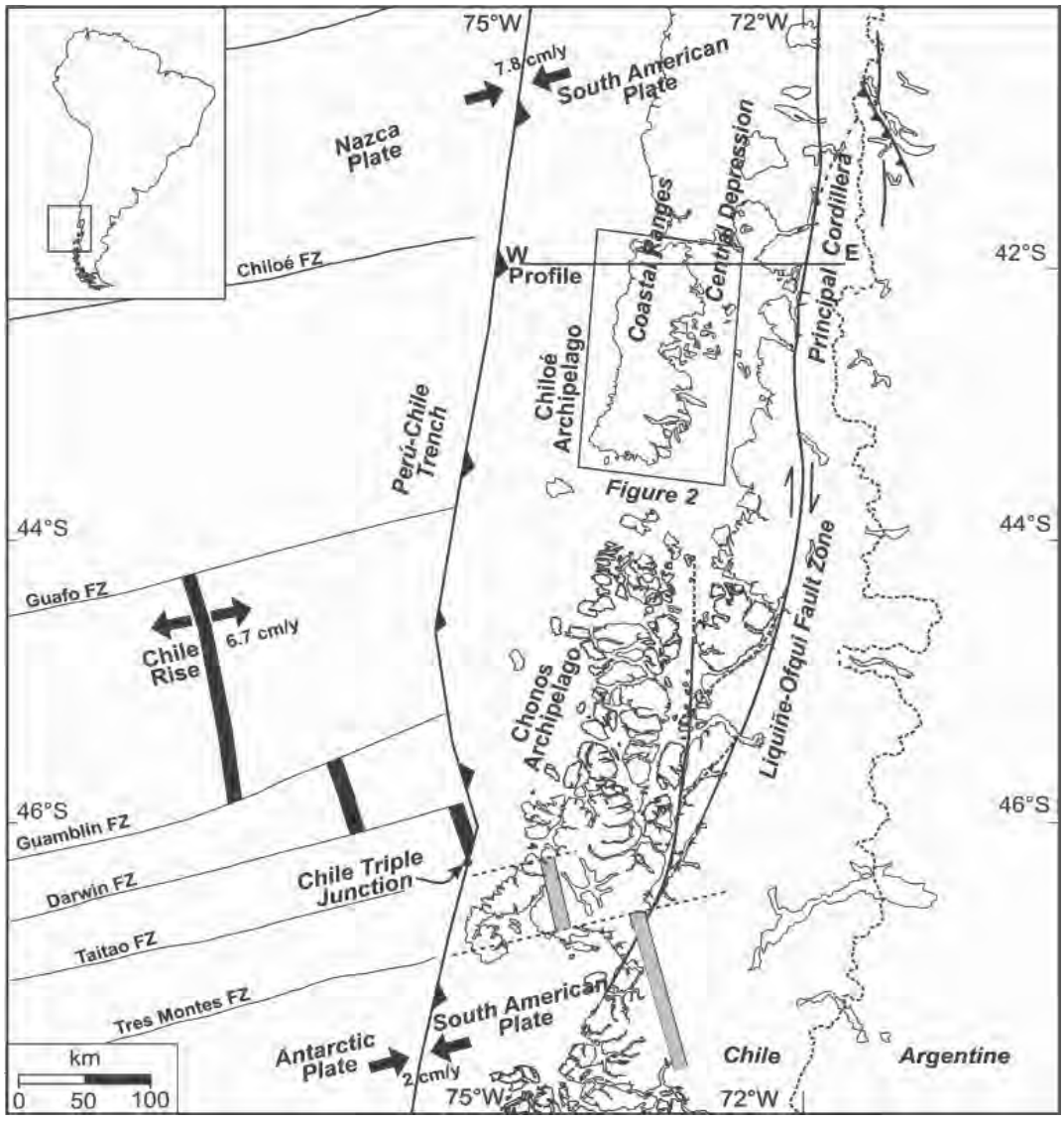

FIG. 1. Tectonic setting of south-central Chile showing major structures, morphologic units, and the area of figure 2 and profile location of figure 3 (modified after Thomson *et al*., 2001). **FZ**: Fracture Zone. Grey bars represented Chile Rise subducted segments.

Aside from two samples for fission-track (FT) dating taken from outcrops near Castro (Thomson and Hervé, 2002), the low temperature history of the metamorphic basement on Chiloé Archipelago remains poorly known. Interpretations for its regional context are extrapolated from studies located further south in the Chonos Archipelago (Hervé *et al*., 2003a), or further north in the locality of Bahía Mansa (Duhart *et al*., 2001). Zircon FT data from three samples in the Valdivia area yielded ages between 176 and 212 Ma, with a weighted average of 186±24 Ma. This last age is interpreted as final cooling below 200°C (Glodny *et al*., 2005).

The Chiloé Archipelago forms part of a forearc high bounding a basin containing approximately 3 km thick sediments of presumably Mesozoic age at its western slope and an approximately 4 km deep intramontane basin of Cenozoic and Pleistocene volcaniclastic and glacial sediments to the east. The basin rocks are affected by steep-dipping inverted extensional faults. The thick succession

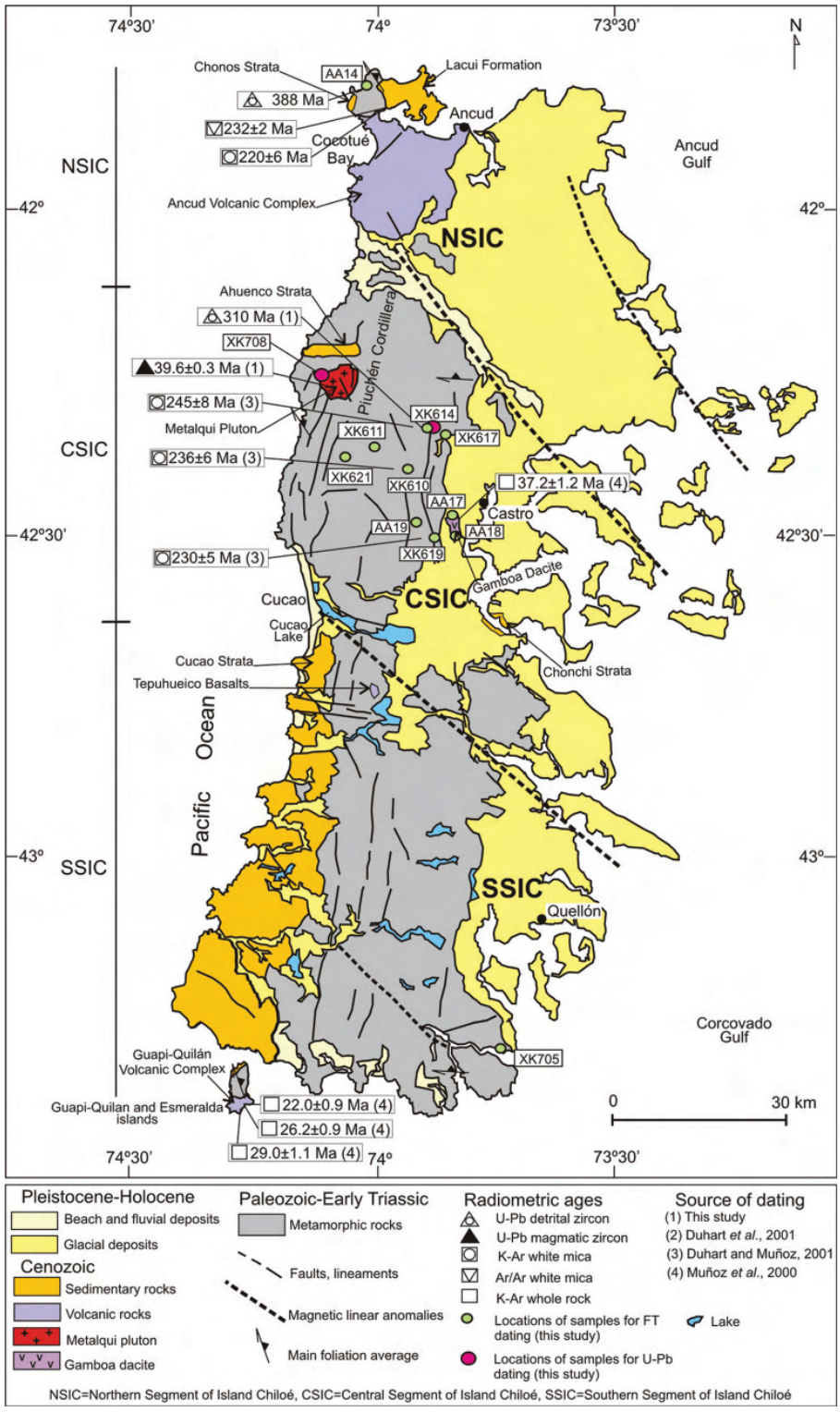

FIG. 2. Geologic sketch map of Chiloé Archipelago (modified from Muñoz *et al*., 1999) showing available U-Pb, K-Ar, and $^{40}Ar/^{39}Ar$ radiometric ages from metamorphic basement rocks, Metalqui Pluton, Gamboa Dacite and Guapi-Quilán Volcanic Complex, and the location of samples for FT dating (modified after Adriasola, 2003).

of sediments in these basins indicates that an important amount of erosion occurred in the region. However, the events that triggered this erosion and sedimentation remain poorly understood.

The aim of this paper is to discuss the low temperature thermal history of the Bahía Mansa Metamorphic Complex with respect to the timing of the major tectonic and magmatic events that affected the basement rocks now located at the forearc high on the Chiloé Archipelago. This report includes 7 zircon and 9 apatite FT ages (with one representative track-length measurement) taken from different segments of the Main Chiloé Island and also the analytical results of two zircon conventional U-Pb determinations of a pelitic schist near the town of Castro and a granitic stock, incompletely published previously (Duhart and Muñoz, 2001; Arenas and Duhart, 2003).

In relation to the ages, in this work the geological time scale of Gradstein *et al.* (2004) is adopted.

2. Geological Framework

2.1. Metamorphic Basement on the Chiloé Archipelago

The oldest rocks of the Chiloé Archipelago form part of the Bahía Mansa Metamorphic Complex (BMMC), defined through stratigraphy, geochronology of sedimentary provenance and metamorphism, and structural relationships along the Coastal Ranges between the southernmost tip of Chiloé Archipelago and ~39°S (Figs. 1 and 2; Duhart *et al.*, 2000, 2001).

The BMMC consists of a heterogeneous group of mainly pelitic to semipelitic schists, metagreywackes, metabasites, some mafic to ultramafic bodies, and, more scarcely, metacherts. Some of these rocks are mylonitic (Duhart *et al*., 2001). The whole unit is characterized by pervasive greenschist facies metamorphism associated with a regional foliation roughly striking in a NW-SE direction, and dipping with moderate angles towards the NE or SW. This foliation is well pronounced in the metasedimentary rocks being defined by mica layers alternating with granoblastic quartz. In the mafic schists foliation is defined by the preferred orientation of amphiboles and in places of epidote. Open symmetric folding of the foliation on all length scales is characteristic for the whole unit, although tight to isoclinal folds and crenulation cleavage have also been reported in outcrops of the northern border of the Main Chiloé Island (Duhart and Muñoz, 2001). Near Ancud, isoclinal folds in quartz veins and albite porphyroblasts with graphite inclusion trails in the metapelitic rocks show the presence of an older foliation (S_1). This means that the dominant foliation is to be regarded as a second foliation (S_2), at least in the metapelites.

Typical mineral assemblage in the metasedimentary rocks are quartz, albite, white mica, chlorite, graphite, sphene, and occasionally garnet and biotite. In the mafic schists the common assemblage is amphibole, epidote, titanite, chlorite, albite, quartz and stilpnomelane, and occasionally garnet. The sporadic occurrence of garnet in metapelites and mafic schists and, biotite in the metapelites suggests higher temperatures within the greenschist facies (biotite grade), possibly reaching amphibolite facies in places. These assemblages were later affected by partial retrograde metamorphism.

For the main metamorphism at Bahía Mansa, Kato and Godoy (1995) reported temperature and pressure conditions of 300 to 400°C and 3 to 4 kbar. A recent study in the Valdivia area (Glodny *et al.*, 2005) indicates that the rocks of the metamorphic basement reached transitional greenschist to blueschist facies metamorphic conditions (420°C and 8-9 kbar). Mineral indicators of high-pressure metamorphism have been reported at other localities within the Coastal Ranges (*e.g.,* Kato, 1985; Kato and Godoy, 1995; Massone *et al.*, 1996, 1998).

Few details are known of the metamorphic conditions of the basement rocks on Chiloé Island. Saliot (1969) and Aguirre *et al*. (1972) have reported the sporadic but widespread occurrence of Na-amphibole and lawsonite as relic minerals within mafic schists on the Main Chiloé Island. These metamorphic assemblages were reported to have formed during an early deformation event (D_1). Na-rich amphibole, phengite and garnet have also been described in the Piuchén Cordillera (Hufmann and Massone, 2000; Hufmann, 2003). White phengitic micas, in pelitic schist are Si-rich, indicative of pressure and temperature conditions of 6-8 kb and 300-400°C for the earlier phase of deformation (Hufmann and Massonne, 2000). Geobarometric studies for metasedimentary rocks from Chiloé Archipelago (Hufmann, 2003) show two *PT*-paths, one of them of a high pressure-low temperature metamorphism (Hufmann, 2003). After high P/T stage substantial heating took place during decompression and the original

features of the blueschist metamorphic facies were obliterated by greenschist metamorphic facies. The high P/T conditions were preserved only in structurally isolated blocks, being considered that they may have reached depths between 23 to 33 km and heated up to a maximum of 450°C (Hufmann, 2003).

A third deformation event D_3 has been described within the CSIC and NSIC, which is characterized by the local crenulation of the S_2 (Duhart *et al.*, 2001). S_2 displays variable orientations in the Main Chiloé Island. It trends east-west in the SE part of the SSIC, whereas NW-SE in the SW part of the same segment as well as within the CSIC and in the NSIC (Fig. 2). Along the eastern flank of the Piuchén Cordillera, an east-west trending S_2 foliation is dominant (Fig. 2).

Geochemical studies in metapelites of the BMMC support a detrital origin derived from the erosion of a continental crust, while the metavolcanic rocks of the BMMC show a basaltic composition of tholeiitic and alkaline affinities with MORB signature (Díaz *et al*., 1988; Crignola *et al.,* 1997). Within the CSIC and SSIC, outcrops of metavolcanic rocks display tholeiitic and calcalkaline affinities with middle oceanic ridge (MORB) and volcanic arc (VAB) basalts signature (Hufmann and Massone, 2000; Hufmann, 2003).

A detailed compilation of U-Pb, K-Ar and $^{40}Ar/^{39}Ar$ isotopic ages for rocks of the BMMC has been published in Duhart *et al.* (2001). The $^{40}Ar/^{39}Ar$ and K-Ar cooling ages constrain the metamorphic peak associated with the main deformation event (D_2) to late Permian-Triassic age, between 260-220 Ma (Duhart *et al*., 2001). Glodny *et al*. (2005) indicate that the prograde metamorphism was followed by progressive penetrative deformation dated by Rb-Sr mineral isochron between 245 to 254 Ma. Older K-Ar and $^{40}Ar/^{39}Ar$ ages (304 and 324 Ma, respectively) obtained by Kato and Godoy (1995) for white mica-bearing blueschist from structurally isolated blocks at Los Pabilos were interpreted as representative of a previous stage of high P/T metamorphism conditions for this region. Recent studies of *PTt* conditions (Willner *et al.*, 2004) suggest that these blocks exhibit metamorphic paths different to other studied portions of the metamorphic basement. In addition, two Rb-Sr mineral isochrons obtained in samples from the same blocks (305.3±3.2 and 296.6±4.7 Ma; Willner *et al.*, 2004) were interpreted as crystallization ages which exceed the maximum cooling ages obtained for other portions of metamorphic basement at the same latitude. Thus, these exotic blocks would have a metamorphic evolution completely different compared to the main volume of metamorphic basement rocks in this area (Willner *et al.*, 2004). Conventional U-Pb dating of detrital zircons indicate maximum possible sedimentation ages between Middle Devonian and early Permian for some components of the BMMC (Duhart *et al*., 2001). Slates with Devonian trilobites have been reported at Buill (Levi *et al*., 1966; Fortey *et al.*, 1992), east of the study area. However these Devonian rocks show different metamorphic style and grade compared to the metamorphic rocks of the Coastal Ranges.

Within the CSIC, three K-Ar ages in white mica (some with biotite traces) determined from metapelites of the Piuchén Cordillera range between 245±8 and 230±5 Ma (Duhart and Muñoz, 2001). Previously published Triassic K-Ar (220±6 Ma) and $^{40}Ar/^{39}Ar$ (232±2 Ma) ages in white mica have been reported on the NSIC (Duhart *et al.*, 1999). These ages are all similar to those reported further north along the Coastal Ranges (Duhart *et al*., 2001). As a whole, these dates are believed to constrain the age of the greenschist facies metamorphism associated with the main deformation event (D_2).

2.2. Sedimentary Cover Successions

The oldest outcrops of continental sedimentary rocks on the Main Chiloé Island are found in the western part of the NSIC (Caleta Chonos Strata) and assigned to the pre-Late Oligocene (Fig. 2; Valenzuela, 1982; Antinao *et al.*, 2000). They consist of up to 120 m thick conglomerates and quartzitic sandstones with some intercalations of fine sandstones displaying plant fossils and coal laminations. The successions are locally intruded by andesitic-basaltic dikes and necks.

Marine sedimentary rocks of Early to Middle Miocene age are well exposed in the western scarps of the NSIC (Lacui Formation) and SSIC (Cucao Strata), and locally along the eastern flank of the Piuchén Cordillera in the CSIC (Chonchi Strata) (Fig. 2; Saliot, 1969; Valenzuela, 1982; Antinao *et al*., 2000; Quiroz *et al*., 2004). Early estimations for the maximum thickness of these units reached up to 800 meters (Tavera *et al.*, 1985), although local

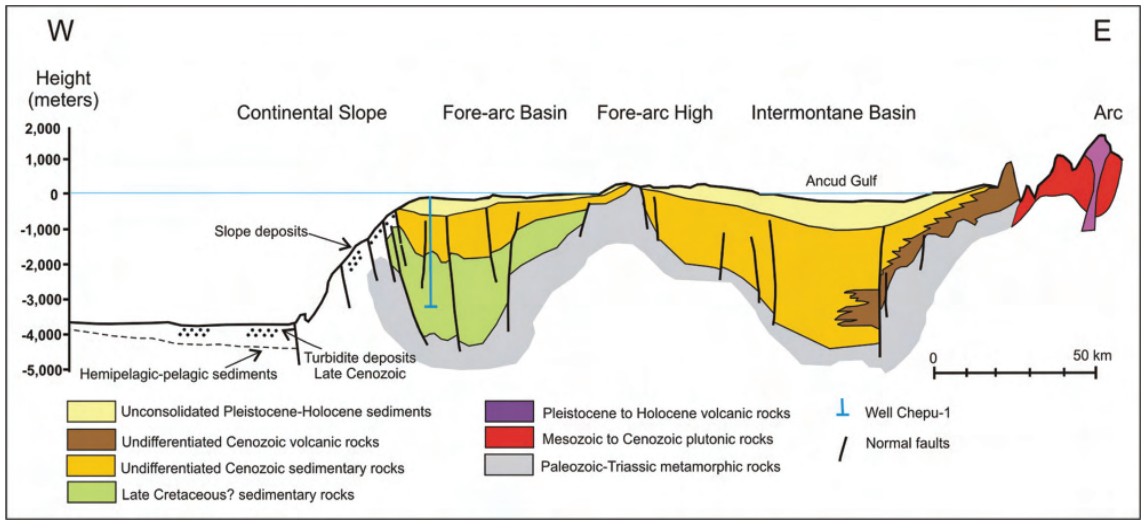

FIG. 3. Geologic profile across the Chilean forearc at latitude 42°S (adapted from González, 1989). At the left, a borehole cuts through fine-grained sandstone and claystone of presumed later Late Cretaceous age (light green), Eocene?-Pliocene sedimentary rocks (dark yellow) and Pleistocene-Holocene sediments (yellow).

outcrops do not exceed 300 m of thickness (Duhart *et al*., 2000). The rocks consist of fine conglomerates and fossiliferous sandstones with fine intercalations of tuffs and mudstones. Early to middle Miocene invertebrate fossils have been described within thin marine layers interbedded in lava flows near of Cocotué Bay (Tavera *et al*., 1985). Parts of these units are chronostratigraphycally equivalent to the marine sedimentary rocks of the Santo Domingo Formation (Martínez and Pino, 1979) deposited in the Valdivia and Llanquihue-Osorno basins (Elgueta *et al*., 2000).

The marine strata are followed by a thin and discontinuous sequence of subhorizontal sandstones and siltstones (Ahuenco Strata) in the northern part of the CSIC (Fig. 2; Arenas and Duhart, 2003), with early Pliocene fossil contents (Watters and Flemming, 1972), equivalent to the Caleta Godoy Formation (Valenzuela, 1982; Antinao *et al.*, 2000) defined along the Coastal Ranges to the west of Puerto Montt.

Mesozoic successions are suspected to be represented below the Neogene strata in the Main Chiloé Island, and scarce roll-overs with remnants of presumably ammonites have been found in the beach of Cucao (Duhart *et al*., 2000). In addition, deep exploratory oil-well and seismic reflection data indicate the presence of a *ca*. 4 km thick forearc basin at the western slope of the Main Chiloé Island, the major part of which has been interpreted to correspond to Mesozoic beds (Fig. 3; González, 1989). The test-wells indicated the stratigraphic succession is composed by two units separated by an unconformity. The upper unit consists of claystone, with intercalations of siltstone, sandstone and conglomerates with abundant volcanic material of Cenozoic age (González, 1989). The *ca.* 3 km lower unit is predominantly built of greywackes of Paleogene or older age and contains intercalations of very fractured siltstone and claystone (González, 1989). The sequence is abruptly interrupted towards the east at the margin of the basin high at the shelf border.

2.3. Cenozoic Volcanic Rocks

An important belt of Cenozoic volcanic rocks crops out along the Chilean Coastal Ranges and Central Depression between 36°S and the Guapi Quilán Island, south of the Main Chiloé Island (Vergara and Munizaga, 1974; Stern and Vergara, 1992). They are interpreted to have been originated during regional extension in response to the subsidence of a thinned crust below the Central Depression (Muñoz *et al*., 2000). The volcanic successions grade towards the Central Depression

into late Oligocene to Miocene continental and marine sedimentary rocks.

In the northern part of the NSIC (Fig. 2), the volcanic rocks consist mainly of well preserved basaltic to andesitic lava flows, dikes, necks with subvertical columnar joints as well as rhyolitic pyroclastic flow deposits, which constitute the Upper Oligocene-Lower Miocene Ancud Volcanic Complex (Muñoz *et al.*, 1999; Antinao *et al*., 2000; Muñoz *et al*., 2000).

Recent field mapping along the northern part of the SSIC has revealed a volcanic succession denominated Tepuhueico Basalts (Quiroz *et al*., 2004). It consists of basaltic to basaltic-andesite lava flows which include abundant vesicles filled by radially fibrous zeolite, quartz and calcite, suggesting hydrothermal activity or very low grade metamorphism. Further south, within the southern part of the Chiloé Archipelago volcanic rocks consist mainly of olivine-clinopyroxene basalts, basaltic andesites and andesites (Guapi Quilán Volcanic Complex); (Muñoz *et al*., 2000). Necks and dikes are well exposed on the Guapi Quilán and Esmeralda Group islands in the southern border of the SSIC (Fig. 2). K-Ar dating in samples of this area range from 22.0±0.9 to 29.0±1.1 Ma (Late Oligocene-Early Miocene) (Muñoz *et al*., 2000).

2.4. Cenozoic Intrusive Rocks

In the CSIC (Fig. 2), isolated outcrops of porphyritic dacites (Gamboa Dacite) have been described as sills and dikes emplaced in Paleozoic-Triassic micaceous schists and dated by K-Ar whole rock in 37.2±1.2 Ma (Muñoz *et al.*, 2000). Due to the gap in time with respect to the Late Oligocene-Early Miocene volcanic rocks in the NSIC, Muñoz *et al*. (2000) proposed that the Gamboa Dacite with older K-Ar ages may represent an earlier, independent magmatic episode, distinct from that which formed the Upper Oligocene-Lower Miocene volcanic belt.

Recent geological surveying has identified an Eocene stock within the northern part of the CSIC (Fig. 2) named as Metalqui Pluton (Arenas and Duhart, 2003). This pluton covers approximately an area of 10 km^2 and exhibits a subcircular shape with branches following the main foliation of the surrounding metamorphic rocks. The rocks show a granular texture and fine to medium grain size. Microscopically, the rocks are holocrystalline with hypidiomorphic to allotriomorphic texture. Rock forming minerals are quartz, plagioclase, K-feldspar, strongly chloritized biotite, amphibole and opaque minerals, with titanite and zircon as accessory minerals.

Towards the north of the Chiloé Archipelago, in the Valdivia area, previous studies have identified scarce and scattered plutons of Late Cretaceous ages (*ca.* 86 Ma; Munizaga *et al*., 1988; Quiroz *et al*., 2006). Towards the south, in the eastern part of the Chonos Archipelago plutons of Early Cretaceous (*ca*. 135 Ma; Pankhurst *et al.*, 1999), Late Cretaceous (*ca.* 76 Ma; Pankhurst *et al*., 1999) and Eocene ages (*ca*. 45 Ma; Pankhurst *et al*., 1999) have been identified. They have been related to the western margin of the North Patagonian Batholith (Munizaga *et al*., 1988; Pankhurst *et al*., 1999). In the southern part of the Chonos Archipelago, in the Taitao Peninsula, small intrusive granodioritic bodies with Pliocene ages (*ca.* 4 Ma; Mpodozis *et al*., 1985; Hervé *et al*., 2003b) have been interpreted as related to the subduction of the Chile Rise segments (Mpodozis *et al.*, 1985; Lagabrielle *et al*., 2000).

2.5. Pleistocene Glacial Deposits

Outcrops of moraines and glaciofluvial deposits are abundant on the eastern side of Chiloé Archipelago (Fig. 2) and characterize the latest advances of the Llanquihue Glaciation (Mercer, 1976; Porter, 1981; Heusser, 1990). The Llanquihue glacial deposits are concentrated along three lobes (Ancud, Castro and Quellón) and their morphology and clast composition suggest that the sediments were transported towards the NW from the Principal Cordillera. Near Puerto Montt, Heusser (1990) estimated a maximum thickness of 1 km for the piedmont glacier that flowed into the Central Depression of the Lake Region. The significant amounts of Cenozoic sediments filling the oceanic trench (González, 1989), the low altitude of the Principal Cordillera, the widespread glacial landscapes and glacial lakes found at these latitudes (Mercer, 1976) imply that the successive Pleistocene glaciations were an important erosion agent along the Southern Andes (*e.g*., Bangs and Cande, 1997; Thomson, 2002).

2.6. Regional Structure

The Main Chiloé Island is subdivided into three main segments separated by important linear magnetic anomalies of NW-WNW orientation (Muñoz *et al*., 1999) along areas of low altitude (Fig. 2). No significant offset along these lineaments has been reported, thus their origin remains controversial.

The segments of the Main Chiloé Island resemble differentially uplifted blocks, the CSIC being the most uplifted and eroded (Duhart *et al*., 2000). These observations are supported by the presence of Eocene plutonic and subvolcanic rocks in the CSIC. The NSIC and SSIC include outcrops of Late Oligocene to Early Miocene subaerial volcanic and Miocene sedimentary rocks. This suggests that differential uplift and erosion occurred since Miocene times.

However, WNW to NW trending magnetic lineaments have been also reported for the basement rocks of the Coastal Ranges further north within the Lake District (~40°S; Duhart *et al*., 1998[1]). These anomalies were related to the parallel strike of magnetite-rich mafic schists with high magnetic susceptibilities (Godoy and Kato, 1990) and, partially, to the tectonic juxtaposition of mafic and pelitic schists (McDonough *et al*., 1997).

A series of North-South to NNE-SSW steep-dipping extensional faults with throw towards the continental platform have been reported along the western scarps of the Main Chiloé Island (Mordojovic and Álvarez, 1977). Seismic profiles and oil-well data across a profile at 42°S show the presence of north-south steep-dipping normal faults that partly accommodate subsequent tectonic inversion of a 4 km thick forearc basin at the western flank of the island (Fig. 3; González, 1989).

From the geological section (Fig. 3) it can be inferred that the steep-dipping normal faults on the island probably developed during an episode of regional extension in the Cenozoic. Numerous K-Ar dates on volcanic rocks of the Coastal Ranges of south-central Chile range between Late Oligocene and Early Miocene, supporting coeval emplacement of magma and subsidence of the Central Depression (Muñoz *et al*., 2000).

Structural inversion accommodated by right-lateral strike-slip reactivation along the forearc during Late Miocene to Pliocene times has been several times proposed as a response to the northwards-oblique subduction of the Nazca Plate beneath South American Plate (Dewey and Lamb, 1992; Beck *et al*., 1993; Rojas *et al*., 1994). Within the arc region, Late Miocene to Pliocene partition into strike-slip and other strain partition along the Liquiñe-Ofqui Fault Zone has been claimed to occur based on microstructural analyses, $^{40}Ar/^{39}Ar$ dating, and zircon and apatite FT thermochronology (Cembrano *et al.*, 2000; Thomson, 2002; Adriasola *et al*., 2006).

3. Geochronology

3.1. U-Pb Analyses

3.1.1. Sample and Methods

In this work the analytical data and the respective concordia diagrams (Table 1; Figs. 2, 4a and 4b) for conventional two U-Pb determinations of detrital (XK614) and magmatic zircons (XK708) separated from rocks located in the CSIC are included, which were only partially reported previously by Duhart and Muñoz (2001) and Arenas and Duhart (2003).

The conventional U-Pb analyses were carried out at the Earth, Atmospheric and Planetary Sciences Laboratory, Massachusetts Institute of Technology (USA). The sample preparation, wet chemistry and mass spectrometry for the U-Pb analyses were done following the procedures described by Schmitz and Bowring (2001).

Sample XK614 is a strongly foliated metapelite composed of alternating lepidoblastic white mica with granoblastic quartz layers. Minor epidote, sphene and detrital zircon crystals are associated preferably within the lepidoblastic mica layers. It represents a metasedimentary component of the BMMC near Castro.

Sample XK708 is a granodiorite composed of quartz, zoned plagioclase and partially altered to sericite, K-feldspar, partially chloritized biotite, scarce amphibole, and opaque minerals. Zircon and sphene are accessory minerals. It corresponds to the Metalqui Pluton emplaced within the metapelitic rocks of the BMMC westwards from Castro.

3.1.2. Zircon U-Pb Results

Four fractions of detrital zircons of the metapelitic sample (XK614) near Castro were analyzed

[1] Duhart, P.; Lara, L.; Pérez, Y.; Rodríguez, C.; Antinao, J.; Clayton, J.; McDonough, M.; Fonseca, E.; Muñoz, J. 1998. Estudio geológico-económico de la X Región Norte. Geología Regional. Servicio Nacional de Geología y Minería, Informe Registrado IR-98-15, 6 Vols., 27 mapas a diferentes escalas.

TABLE 1. ZIRCON U-Pb RESULTS FOR THE CASTRO METAPELITE AND METALQUI PLUTON.

				Isotopic ratios									Dates (Ma)					
Sample (a)	Pb^*/Pb_c (b)	Pb_c (Pg) (c)	Th/U (d)	$^{206}Pb/^{204}Pb$ (e)	$^{208}Pb/^{206}Pb$ (f)	$^{206}Pb/^{238}U$ (f)	%err (g)	$^{207}Pb/^{235}U$ (f)	%err (g)	$^{207}Pb/^{206}Pb$ (f)	%err (g)	corr. coef.	$^{206}Pb/^{238}U$ (h)	± (i)	$^{207}Pb/^{235}U$ (h)	± (i)	$^{207}Pb/^{206}Pb$ (h)	± (i)
XK614																		
z1	6.7	6.9	0.39	438	0.122	0.066194	0.57	0.502239	0.66	0.055029	0.31	0.88	413.2	2.3	413.2	2.2	413.4	6.9
z2	51.6	0.8	0.37	3307	0.120	0.061971	0.12	0.466839	0.18	0.054636	0.14	0.66	387.6	0.4	389.0	0.6	397.4	3.0
z3	10.4	8.5	0.36	676	0.114	0.049364	0.31	0.358134	0.45	0.052618	0.31	0.72	310.6	0.9	310.8	1.2	312.3	7.0
z4	3.1	54.2	0.44	211	0.132	0.057671	0.24	0.424895	0.93	0.053434	0.85	0.43	361.4	0.8	359.5	2.8	347.3	19.3
XK708																		
z1	8.1	1.0	0.36	540	0.118	0.006156	0.40	0.040211	0.74	0.047373	0.60	0.59	39.6	0.2	40.0	0.3	68.1	14.3
z2	7.9	2.0	0.45	513	0.144	0.006153	0.40	0.039792	0.75	0.046903	0.61	0.59	39.5	0.2	39.6	0.3	44.2	14.5
z3	0.2	44.0	0.29	33	0.097	0.005833	1.24	0.039764	5.82	0.049444	5.41	0.42	37.5	0.5	39.6	2.3	169.0	126.4
z4	8.6	2.3	0.47	553	0.152	0.006164	0.37	0.039819	0.85	0.046848	0.72	0.53	39.6	0.1	39.6	0.3	41.5	17.3

a. z1, z2, z3, and z4 are labels for fractions composed of single grains of zircon; **b.** Ratio of radiogenic Pb to common Pb; **c.** Total weight of common Pb; **d.** Model Th/U ratio calculated from radiogenic $^{208}Pb/^{206}Pb$ ratio and $^{207}Pb/^{206}Pb$ age; **e.** Measured ratio corrected for spike and fractionation only. Mass fractionation corrections were based on analysis of NBS-981 and NBS-983; Correction of 0.25±0.04 %/amu (atomic mass unit) was applied to single-collector Daly analyses; **f.** Corrected for fractionation, spike, blank, and initial common Pb. All common Pb was assumed to be procedural blank; **g.** Errors are 2 sigma, propagated using the algorithms of Ludwig (1980); **h.** Calculations are based on the decay constants of Jaffey *et al.* (1971); **i.** Errors are 2 sigma.

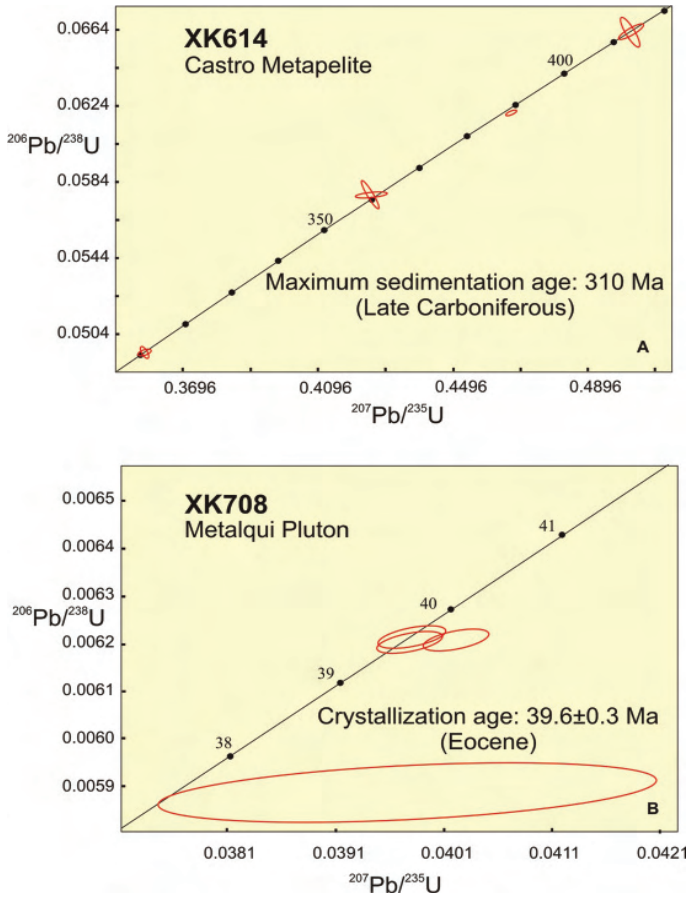

FIG. 4. U-Pb concordia diagrams for samples XK614 and XK708. **A.** Castro Metapelite with concordant ages at 310, 360, 390 and 412 Ma. The minimum age is considered the maximum possible sedimentation age; **B.** Metalqui Pluton with two concordant ages. The best estimate of crystallization age is the mean of $^{206}Pb/^{238}U$ dates of two concordant analyses of 39.6±0.3 Ma with a mean squared weighted deviate (MSWD) of 0.2.

(Table 1). They are concordant at 310, 360, 390 and 412 Ma (Fig. 4a). The youngest obtained age of 310 Ma is interpreted as the maximum possible sedimentation age, in the Late Carboniferous, whereas the other ages indicate a sediment provenance from the erosion of Devonian zircon-bearing rocks.

Four fractions of magmatic zircons separated from the sample of the Metalqui Pluton (XK708) were analyzed (Table 1). Two fractions are concordant and the other two are discordant (Fig. 4b). The best estimate of crystallization age is the weighted mean of $^{206}Pb/^{238}U$ dates of two concordant analyses of 39.6±0.3 Ma with a mean squared weighted deviate (MSWD) of 0.2. The discordant fractions can be due to Pb loss processes during younger events.

3.2. Fission Track Analyses

3.2.1. Methodology

Four samples from the BMMC for fission track (FT) thermochronology were obtained during one field season to Main Chiloé Island in summer 2001, whereas the Sernageomin (Servicio Nacional de Geología y Minería) Puerto Varas office provided seven additional separates of zircon and apatite from previous field campaigns to the Piuchén Cordillera. At the Rühr-University of Bochum (Germany), the separated minerals were mounted, polished, and etched according to the techniques outlined by Hurford *et al*. (1991). The total etching times for the zircon samples from this study varied between 9 and 17 h and were achieved at steps varying

TABLE 2. FISSION TRACK RESULTS FROM THE CHILOÉ ARCHIPELAGO.

Sample number	Location GPS coordinates†	Rock type	Mineral	Number of crystals	Track density ($x10^6$ tr.cm^{-2})			Age dispersion ($P(\chi^2)$)	Central age (Ma) (±1σ)	Apatite mean track length (μm±1σ)	No. of confined tracks	Standard deviation (μm)
					ρ_s (N_S)	ρ_i (N_i)	ρ_d (N_d)					
AA14	Chiloé, Guabún 41°47'27''S; 74°03'24''W	Micaschist	Apatite**	16	0.6426 (134)	3.040 (634)	1.591 (10991)	43%(0%)	67.0±10.7	-	-	-
			Zircon*	14	13.52 (2633)	2.188 (426)	0.3890 (5335)	11%(14%)	155.6±10.1			
AA17	Chiloé, Gamboa Alto 42°51'51''S; 73°51'51''W	Dacite	Apatite**	20	0.1563 (104)	1.599 (817)	1.599 (11043)	1%(69%)	33.9±3.6	13.66±0.28	30	1.53
			Zircon*	20	6.4114 (5464)	4.345 (3864)	0.3923 (5417)	7%(4%)	36.0±1.2			
AA18	Chiloé, Gamboa Bajo 42°27'21''S; 73°50'30''W	Dacitic porphyry	Apatite*	20	0.1766 (69)	1.331 (520)	1.607 (11095)	1%(82%)	36.1±4.7	-	-	-
			Zircon*	20	4.901 (4758)	3.778 (3668)	0.3785 (5227)	3%(46%)	35.4±1.1			
AA19	Chiloé, Gamboa Alto 42°27'33''S; 73°53'45''W	Micaschist	Zircon*	20	10.36 (5637)	2.218 (1207)	0.3864 (5336)	13%(2%)	117.9±5.9	-	-	-
XK610	Chiloé, Castro 42°23'17''S; 73°52'56''W	Micaschist	Apatite**	20	0.0773 (14)	0.2322 (42)	1.628 (13144)	4%(79%)	91.5±28.3	-	-	-
XK611	Chiloé, Castro 42°21'46''S; 73°55'17''W	Micaschist	Apatite**	12	0.0827 (8)	0.2896 (28)	1.635 (13306)	0%(95%)	78.8±31.7	-	-	-
			Zircon**	20	10.84 (6390)	2.015 (1188)	0.3798 (5245)	5%(16%)	131.8±5.2			
XK614	Chiloé, Castro 42°19'25''S; 73°50'28''W	Micaschist	Apatite**	13	0.2334 (39)	0.9455 (158)	1.642 (13498)	41%(15%)	77.0±18.6	-	-	-
XK617	Chiloé, Castro 42°20'08''S; 73°48'23''W	Micaschist	Apatite**	20	0.0877 (12)	0.4901 (67)	1.649 (13690)	0%(97%)	49.9±15.7	-	-	-
XK619	Chiloé, Castro 42°29'41''S; 73°48'35''W	Micaschist	Apatite**	15	0.1998 (32)	0.7928 (127)	1.656 (13881)	21%(72%)	75.0±16.1	-	-	-
			Zircon**	30	9.450 (8378)	2.616 (2319)	0.3883 (5363)	15%(0%)	90.9± 3.9			
XK621	Chiloé, Piuchén 42°22'50''S; 73°59'20''W	Micaschist	Apatite**	19	0.1303 (18)	0.490 (62)	1.670 (14265)	1% (96%)	81.7±21.9	-	-	-
XK705	Chiloé, San Pedro island, 43°17'44''S; 73°39'54''W	Micaschist	Zircon**	10	8.405 (2542)	2.020 (611)	0.4247 (5865)	34%(0%)	103.0±12.4	-	-	-

Analyses by the external detector method using 0.5 for the $4\pi:2\pi$ geometry correction factor. $P(\chi^2)$ is the probability of obtaining a $\chi 2$ value for (μ-1) degrees of freedom, where μ is the number of crystals. *Apatite FT ages calculated by A.C.A. using dosimeter glasses CN5 with ζ_{CN5}=333.9±7.3 and zircon FT ages using CN2 glasses with ζ_{CN2}=129.9±1.64. **Apatite FT ages obtained by A.C.A. using dosimeter glasses CN5 with ζ_{CN5} =333.3±8.2 and zircon FT ages using CN2 glasses with ζ_{CN2} =130.7±1.9. † South American Provisory Datum, 1956.

between 1 and 4 h. FT analysis was performed using the external detector method (Naeser, 1976) and the calibration approach of Hurford and Green (1983), and irradiated in the Risø reactor of the National Laboratory at Roskilde, Denmark, and at the Oregon State University TRIGA Reactor, in Corvallis, USA. The neutron flux was monitored using uranium-dosed Corning glasses CN5 for apatite and CN2 for zircon. Zircon packages (RU21 and RU24) were irradiated with a total neutron flux of 1.0 x 10^{15} n·cm^{-2}. Apatite packages (RUA15 and RUA16) were irradiated each with a total neutron flux of 1.2 x 10^{16} n·cm^{-2}. FT densities were counted using a Zeiss Axioplan microscope at 1250x magnification. Apatite FT lengths were measured using an attached drawing tube and digitizing tablet calibrated against a stage micrometer, following the recommendations of Laslett *et al*. (1982). Central ages (Galbraith and Laslett, 1993) were calculated using the International Union of Geological Sciences (IUGS) recommended ζ-calibration approach of Hurford and Green (1983). ζ-calibration factors were obtained with the Fish Canyon (apatite and zircon), Durango (apatite), Mount Dromedary (apatite and zircon), Buluk (zircon), and Tardree (zircon) age standards (Hurford, 1990). A total of 9 apatite and 7 zircon FT ages, plus one available confined track-length measurement from one apatite sample are reported in this paper and displayed in table 2.

3.2.2 Fission Track Results from the Metamorphic Basement on Main Chiloé Island

The distribution of the fission track central ages is shown in figure 5. In particular, for most of the apatites (of detrital and metamorphic origin) and for zircon sample XK705 high age dispersions or large relative errors accompanied the central ages. For apatites this is probably due to their low-uranium contents (*i.e.,* few spontaneous tracks) and their frequently rounded or incomplete surfaces. In some cases, the abundant presence of inclusions impeded any age determination. For zircons, the main factor for the variability in FT retention appears to be radiation damage by alpha decay, which causes a decrease in FT retentivity (Kasuya and Naeser, 1988; Nasdala *et al*., 2001). This effect is considered to be dependent of the variable concentrations of U, Th, and He in time (see discussion in Reyners and Brandon, 2006). At geologic timescale, alpha damage is able to persist to high temperatures where it reduces the retentivity of associated fission tracks. The presence of fluids, or individual variations within trace-element constituents are additional problems affecting the distribution of spontaneous tracks (and hence the reproducibility of the central age) within a sample and which remain poorly understood. A common practice in FT analysis is that when the relative age dispersion exceeds 20%, the concept of a single central age is meaningless and analyses are extended in discerning between single-grain age populations (*e.g.,* Galbraith and Green, 1990). Therefore the results are presented and discussed separately with histograms and radial plots for zircons and apatites along the following sections.

The grain-age component analyses were assessed using the Software Binomfit (Brandon, 2002). This program creates probability-density distribution plots which are obtained based on the binomial peak-fitting algorithm of Galbraith and Green (1990). In general, this consists of searching for the best fit solution by directly comparing the distribution of the grain data to a predicted mixed binomial distribution, estimated by maximum likelihood. The best-fit peaks are reported by age, uncertainty, and size, and are shown in tables 3 and 4. The uncertainty of the individual peaks is described here within 68% confidence interval (C.I., approximately equivalent to 1 σ error). The size of the individual peaks is reported as a fraction (in percent). The algorithm has proved to be a successful tool for interpreting grain-age populations of samples with mixed FT ages in a wide range of denudational studies, such as detrital thermochronology (*e.g.,* Brandon *et al.*, 1998; Reyners and Brandon, 2006). Note that the confidence intervals for the FT ages are generally asymmetric, with the older interval being larger than the younger interval. For samples with one peak, the median FT age represents a pooled age that resembles the central age of Galbraith and Laslett (1993).

3.2.3. Zircon FT Results

For the rocks of the metamorphic basement, the zircon samples yield central FT ages between Late Jurassic (155.6±10.1 Ma) and Late Cretaceous (90.0±3.9). The oldest zircon FT ages were obtained from the NSIC and CSIC, whereas younger ages were obtained at the eastern flank of Piuchén Cordillera in the CSIC.

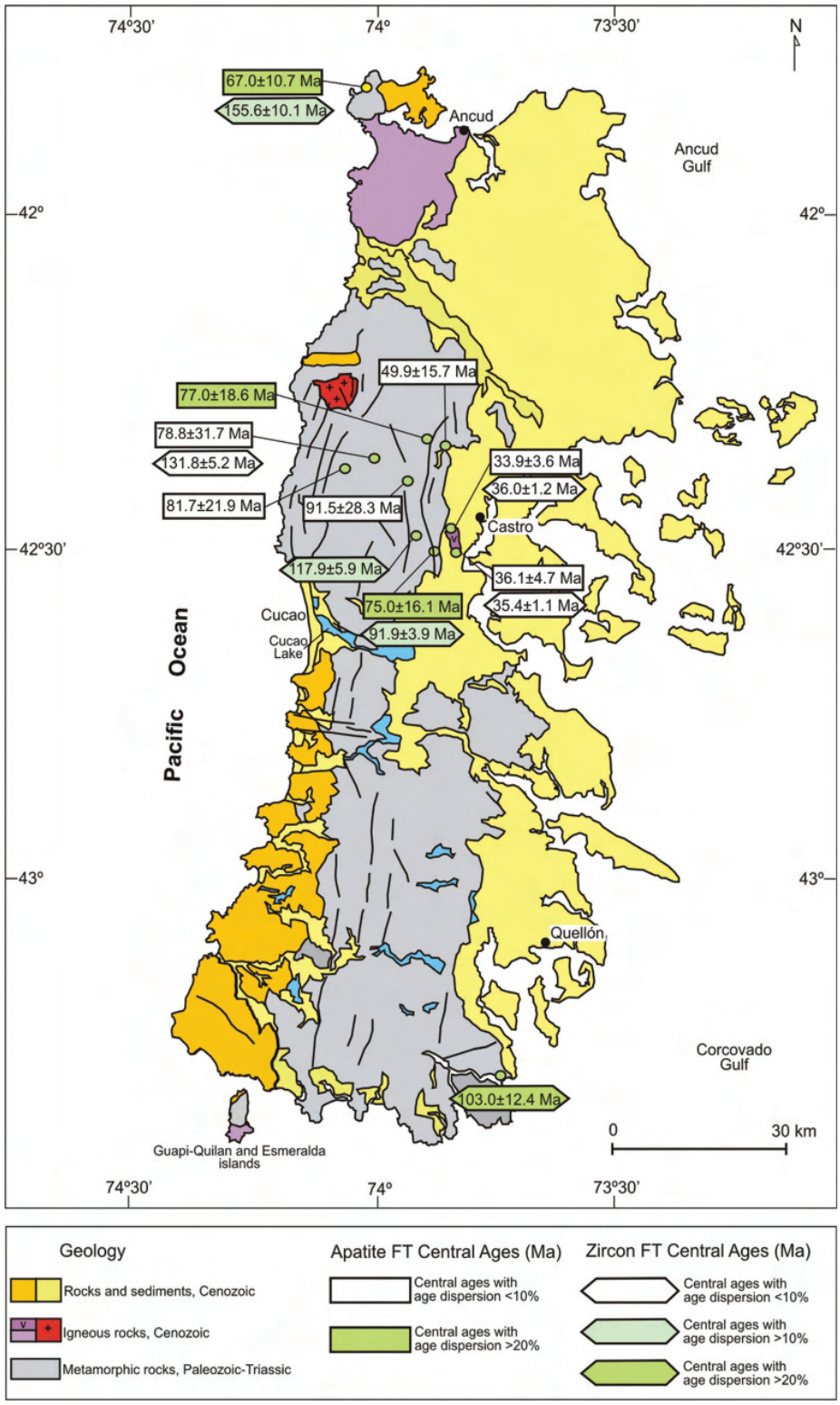

FIG. 5. Location of fission track central ages on the Main Chiloé Island. See geological explanation in figure 2. Refer to text for discussion on the sample age dispersions.

TABLE 3. FISSION TRACK AGE-COMPONENT MODELLING RESULTS FOR ZIRCON SAMPLES OF THE BMMC.

Sample number	Location	Nt	Deconvoluted peaks (Ma)	68% Confidence interval (Ma)		Fraction (%)	P(χ2)	P(F)
AA14	Chiloé, Guabún	14	140.9 198.8	-12.0 -25.6	+13.1 +29.3	67.1 32.9	12%	1%
AA19	Chiloé, Gamboa Alto	20	79.3 114.5	-10.4 -11.5	+12.0 +12.8	11.7 88.3	19.5%	<1%
XK611	Chiloé, Castro	20	132.1	-4.8	+5.0	100	25%	<1%
XK619	Chiloé, Castro	30	83.0 120.0	-3.8 -12.4	+3.9 +13.9	77.3 22.7	27%	<1%
XK705	Chiloé, San Pedro Island	10	79.7 163.4	-5.0 -11.3	+5.3 +12.1	59.7 40.3	10%	<1%

Notes: **P(χ2)** =χ2 probability for concordance of grains. Peak ages calculated using the binomial peak-fit method (Galbraith and Green, 1990). **P(F)**: probability that the improvement of fit associated with inclusion of an older peak in the peak-fit model could be due to random chance alone. **Nt**: total number of grain ages in peak. **Fraction (%)**: percent of total number of dated grains in an individual peak. Initial guess parameters for the binomial peak-fit iterations were chosen randomly by the Software Binomfit (Brandon, 2002).

Sample AA14 (Fig. 6), from the NSIC, yielded a zircon FT central age 155.6±10.1 Ma, and an age dispersion of 11% (Table 2). Although not sufficient to interpret as a discordant grain age distribution, the analysis of its component ages revealed two grain-age populations of 140.9 Ma (C.I. +13/-12 Ma; 67.1%) and 198.9 Ma (C.I. +29.3/-25.6 Ma; 32.9%) (Table 3).

Samples AA19, XK611, and XK619 from the CSIC yielded Early to Late Cretaceous zircon FT ages. Sample XK611 indicated an Early Cretaceous central age of 131.8±5.2 Ma and a small age dispersion of 5% (Table 2). Sample AA19 (Fig. 6) showed a central age of 117.9±5.9 Ma, and an age dispersion of 13% (Table 2). The analysis of its single grain-age distributions revealed two grain-age populations: Late Cretaceous (79.3 Ma; C.I. +12.0/-10.4 Ma; 11.7%) and Early Cretaceous (114.5 Ma; C.I. +12.8/-11.5 Ma; 83.3%) (Table 3). For sample XK619 (Fig. 6) its central age of 90.9±3.9 Ma showed a high age dispersion of 15% (Table 2), revealing two single grain-age populations dated at 120 Ma (C.I. +13.9/-12.4 Ma; 22.7%) and 83 Ma (C.I. +3.9/-3.8 Ma; 77.3%) (Table 3).

Sample XK705 (Fig. 6) corresponds to the southernmost segment of the Main Chiloé Island. Only 12 grains were dated and its central FT age of 103.0±12.4 Ma is accompanied by a large age dispersion of 34% (Table 2) indicating a discordant grain-age distribution. The analyses of the single grain-age spectra indicated two grain-age populations with peaks at 163.4 Ma (C.I. +12.1/-11.3 Ma; 40.3%) and 79.7 Ma (C.I. +5.3/-5.0 Ma; 59.7%) (Table 3).

Establishing the temperature range in which fission tracks in zircon disappear or totally anneal is difficult. The Zircon Partial Annealing Zone (ZPAZ, Tagami and Shimada, 1996) is a temperature range that depends on the cooling rate of the sample, the effect of α-radiation damage for individual zircon grains (which is dominated by the decay path of ^{238}U, Th and diffusivity of He), and variations in color or internal chemistry (*e.g.,* Rahn *et al*., 2004; Reyners and Brandon, 2006). Tagami and Shimada (1996) estimated that annealing effectively occurs within a temperature range of between 220 and 350°C for cooling rates between 10 and 100°C/km. For pristine magmatic zircons higher temperatures are required for total annealing, whereas lower temperature ranges are expected for α-damaged zircons.

Figure 6 shows the graphic analyses of zircons from basement rocks of the study area. Although variable accumulated α-damage in zircon is commonly cited as being the third major factor -after temperature and time- affecting the retentivity of fission tracks in this mineral (*e.g.,* Brandon *et al.* 1998; Rahn *et al.* 2004; Reyners and Brandon, 2006), we do not observe any tendency in the plots of U content *versus* single-grain age. With the exception of samples AA14 (of Jurassic central age with relatively low dispersion) and XK705 (which had only 10 dated grains), most of the probability-

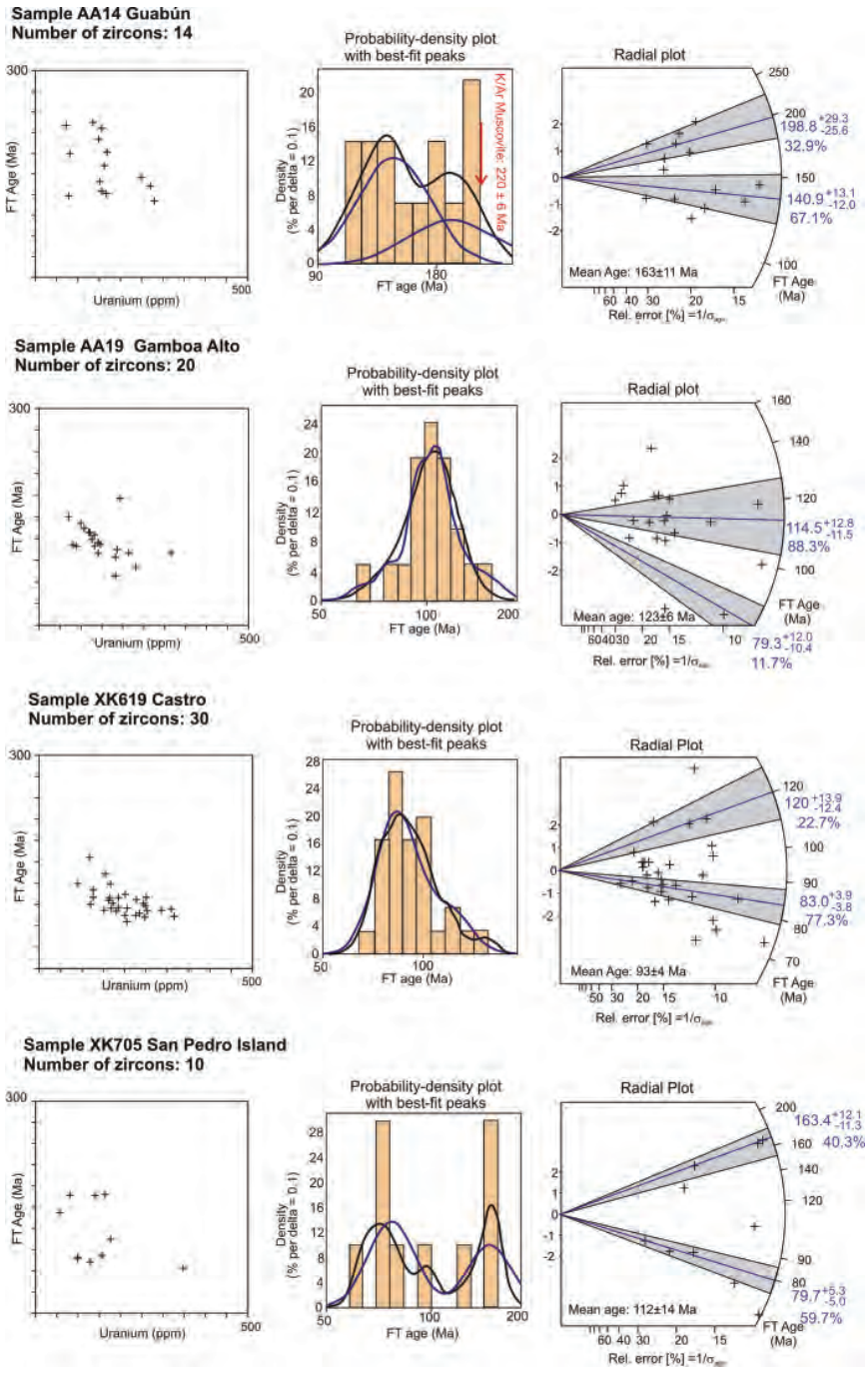

FIG. 6. Graphic analyses of zircon FT grain-age distributions for 4 samples of micaschists from different areas of the Main Chiloé Island. The central charts are probability-density plots (Brandon, 2002) with their respective probability-density distribution curves (black) and estimated component distributions (blue lines) by the binomial peak-fit method (Brandon, 1996). The best fits or peaks are shown in the Radial Plots (Galbraith and Laslett, 1993) together with their error at a 68% confidence interval and their relative proportion. At the right, the graphs at the left side show the variable distribution of FT age *versus* uranium content for each individual zircon grain suggesting little effect of α-radiation damage in the minerals (*e.g.*, Rahn, 2004). The plots indicate a tendency of cooling from temperatures below ~300°C in Early to mid Cretaceous times, with the exception of samples AA14 and XK705. Refer to discussion in text.

TABLE 4. FISSION TRACK AGE-COMPONENT MODELLING RESULTS FOR APATITE SAMPLES OF THE BMMC.

Sample number	Location	Nt	Deconvoluted peaks (Ma)	68% Confidence interval (Ma)		Fraction (%)	P(χ2)	P(F)
AA14	Chiloé, Guabún	16	37.6 89.6	-7.5 -21.0	+9.4 +27.4	32.9 67.1	16%	<1%
XK610	Chiloé, Piuchén Cordillera	16	91.4	-24.2	+32.9	100	10%	<1%
XK617	Chiloé, Piuchén Cordillera	20	43.9	-9.4	+12.0	100	19%	<1%
XK621	Chiloé Piuchén Cordillera	19	52.5 109.9	-14.6 -34.9	+20.2 +51.0	49.5 50.5	15%	1%
XK611	Chiloé, Castro	12	78.8	-26.0	+38.6	100	4%	<1%
XK619	Chiloé, Castro	12	68.5	-11.5	+13.9	100	9%	<1%

density plots indicated single peaks towards early Late Cretaceous. We speculate that the variable annealing suspected in these samples may have some other cause, perhaps related to chemical variation of individual crystals within the sample rocks while being subjected to the local effect of magmatic heat input or fluids. This effect would result in high age dispersions indicated by the younger grain-age components found in their FT age spectra. A thermal event postdating the metamorphic cooling of the basement could partially reset rocks at depths beneath or within the ZPAZ.

Despite these considerations, the central FT ages of zircons are generally mid to Late Cretaceous independent of the structural position in the island, and therefore probably represent the onset of cooling from depths sufficient to reset fission tracks, roughly at temperatures equivalent to depths of ~10 to 12 km (*e.g.* Brandon *et al.*, 1998; see discussion in Adriasola *et al*., 2006).

It should be noted that the zircon FT central ages are generally at least ~100 Myr younger than the K-Ar ages of the white micas representing widespread metamorphism in the greenschist facies on Chiloé Archipelago (Duhart and Muñoz, 2001), and only the oldest single grain component ages are close to the ages of metamorphism for these rocks (*e.g.,* sample AA14, Fig. 6).

It can be speculated that the older grain-age components represent cooling after deformation phase D_3. This is represented by crenulation cleavage and refolding of S_2 rocks in the greenschist facies. However, more structural and geochronological data are necessary to support this interpretation.

3.2.4. Apatite FT Results

Apatite FT central ages from the metamorphic basement were obtained only in samples from the NSIC and CSIC. These range between Early Cretaceous (117.9±5.9 Ma) and Eocene (49.9±15.7 Ma). Unfortunately most of the dated grains had few spontaneous tracks and no statistically representative track-length measurement could be obtained from them. Nevertheless a tendency to yield Late Cretaceous ages and locally Eocene ages was observed for the basement rocks of the CSIC.

Because of their low U concentrations, to obtain a more substantial interpretation of the apatite FT cooling histories we would have needed more grains and better samples to date. With the available data, the approach for constraining their age dispersions was to study their grain-age populations with probability-density plots from Binomfit (Brandon, 2002). The results of the modelling are shown in table 4 and graphically displayed in figure 7. The aim of the analysis was to discriminate very young and very old component ages with no geological meaning.

The most problematic sample XK614 (Fig. 7), showed two populations: a younger one with 63.9 Ma (C.I. +15.3/-12.4; 84.9%) and an older component of 213.2 Ma (C.I. +282.0/-122.6 Ma; 15.1%)

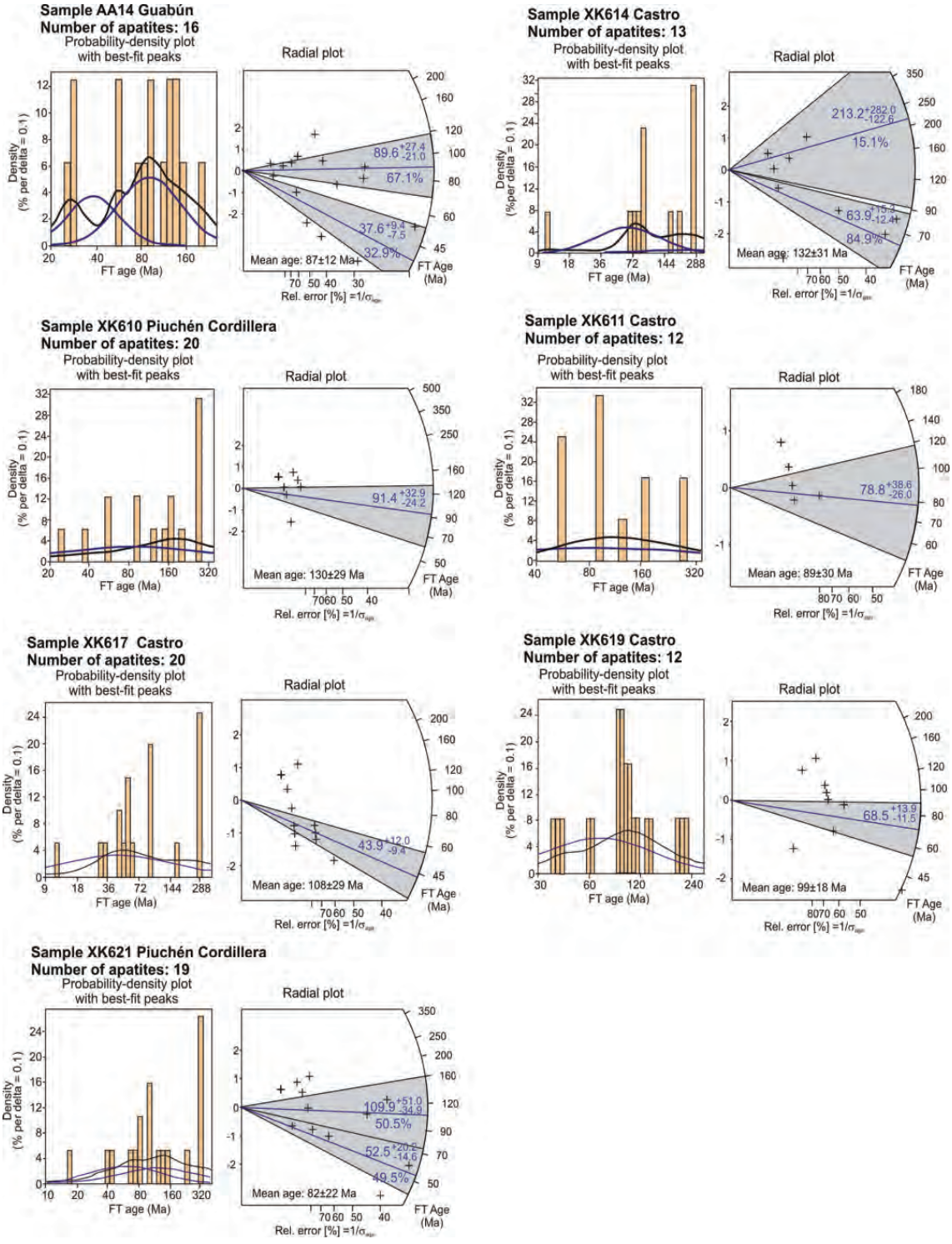

FIG. 7. Radial plots (Galbraith, 1990) and probability-density distribution plots (Brandon, 2002) for 7 apatite samples with discordant single grain FT-age distributions. These indicate a tendency to monotonic cooling ages from Late Cretaceous to Eocene times. The very young and very old single grain-ages are interpreted as a poor resolution effect due to the few spontaneous tracks in the apatite grains. Refer to figure 6 for legend.

(Table 4) overlapping in error within 1σ error to zircon FT ages from similar outcrops or even ages of metamorphism determined in the area.

Very young apatite ages (*e.g.*, 'zero ages' or grains without any track) should be excluded as well, because this would imply exhumation from depths exceeding 4 km (assuming a constant geothermal gradient of ~30°C/km) in very recent times. The latest Miocene-Pliocene regional uplift event recorded by the <1 km thick exposure of Cenozoic marine strata on the Main Chiloé Island (Tavera *et al.*, 1985) does not seem to be enough for exposing rocks at temperatures within the Apatite Partial Annealing Zone (APAZ). The low track density in the apatite samples instead probably reflects their low U concentration (Fig. 7).

Sample AA14 (Fig. 7) from the NSIC yielded a poorly constrained FT central age of 67±11 Ma with a very high age dispersion of 43% (Table 2). The analysis of its component ages revealed two grain-age populations of 90 Ma (C.I. +27.4/-21.0 Ma; 67.1%) and 38 Ma (C.I. +9.3/-7.5 Ma; 32,9%) (Table 4).

Samples XK610, XK614, XK617, XK619 and XK0621 from the CSIC yielded poorly defined Late Cretaceous to Eocene central ages. The oldest apatite FT central ages from this segment were obtained from samples XK610 and XK621, respectively of 92±28 and 82±22 Ma (Table 2). The probability-density plot of sample XK621 (Fig. 7) showed two components: an older Early Cretaceous (110 Ma; C.I. +51/-35 Ma; 50.5%) and a younger Eocene peak (52.5 Ma; C.I. +20.2/-14.6 Ma; 49.5%) (Table 4). Late Cretaceous to Eocene single peaks were obtained for all of the other samples of the CSIC (see Fig. 7 and Table 4).

The youngest apatite FT central ages were obtained from samples XK617 and XK619 (Fig. 7), of respectively 49.9±15.7 and 75.0±16.1 Ma (Table 2). Despite both samples carried large age dispersions (>10%), their probability-density distribution plots indicated a tendency to single grain-age populations. The deconvoluted FT age of sample XK617 was 43.9 Ma (C.I. +12.0/-9.4 Ma) (Table 4), whereas of sample XK619 was 68.5 Ma (C.I. +13.9/-11.5 Ma) (Table 4). The large errors accompanying their ages is due to the few spontaneous tracks found in the surfaces of the grains.

In general, these rocks indicate cooling at temperatures below ~100°C in Late Cretaceous to Eocene times. Cooling rates cannot be determined from the apatite FT data due to the few available track-length measurements. Nevertheless one previously analyzed sampled near Castro indicated rapid monotonous cooling at 67±7 Ma (Thomson and Hervé, 2002).

We infer that the younger Eocene apatite FT component ages detected in samples of the Piuchén Cordillera could reflect partial resetting by magmatism. This implies that the rocks were near to the surface or within depths equivalent to the temperature range of the APAZ at the moment they were thermally reset. The younger Eocene ages are as well concordant to the emplacement age of the Metalqui Pluton in the CSIC.

3.2.5. Samples from Cenozoic Volcanic Rocks

Four zircon and apatite FT ages from samples AA17 and AA18 correspond to porphyric dacites from the CSIC near Castro (Fig. 2). The zircon and apatite FT ages yielded values of between 36.0±1.2 Ma and 33.9±3.6 Ma (Table 2 and Fig. 5), overlapping in age within 1 σ error. The similar ages despite their different closure temperatures are compatible with rapid cooling at ~36 Ma. Confined track length measurements for sample AA17 indicate a long mean track length (13.7±0.8 μm), supporting rapid cooling below 120°C (*e.g.,* Green *et al.*, 1989). The data support a late Eocene age of emplacement for the subvolcanic complex in the CSIC reported previously by Muñoz *et al*. (2000).

4. Discussion

Previous studies of the BMMC using U-Pb conventional detrital zircon geochronology indicated within the NSIC concordant ages of 388, 462, 465 and 1,120 Ma (Duhart *et al*., 2001). These dates constrain the maximum sedimentation age for this portion of the BMMC to the Middle Devonian (Duhart *et al.*, 2000, 2001). In addition, these data suggest primary zircon sources of Devonian, Ordovician and Mesoproterozoic ages.

K-Ar and $^{40}Ar/^{39}Ar$ dating of white micas from metapelitic schists of the same locality yielded 220±5 and 232.5±2.7 Ma, respectively (Duhart *et al.*, 2000, 2001). The latter were interpreted to indicate the onset of cooling following greenschist facies metamorphism associated to the main phase of deformation (D_2).

Three additional samples for K-Ar dating of white mica -some of which included traces of biotite- taken from metapelitic rocks of the CSIC near Castro, yielded 236±6, 245±8 and 230±5 Ma, respectively (Duhart and Muñoz, 2001). These cooling ages are in good agreement to those previously reported from the NSIC, supporting that both segments of the BMMC were affected by greenschist facies metamorphism during the Middle to early Late Triassic. In this work we report concordant U-Pb detrital zircon ages of 310, 360, 390 and 412 Ma from sample XK614 located in the CSIC, which indicates an Late (Pennsylvanian) Carboniferous maximum age of deposition for this portion of the BMMC in the Chiloé Archipelago, and which also suggests primary zircon sources of Carboniferous and Devonian ages.

The available detrital zircon concordant ages dataset shows Carboniferous, Devonian, Ordovician and Mesoproterozoic primary zircon sources. The detrital zircons probably derived from magmatic sources in adjacent or distal areas or, alternatively, they may represent recycled zircons. If we assume a magmatic source for the sediments prior to metamorphism, the Carboniferous zircons (310 Ma) could have been derived from the north by erosion of the batholiths of Futrono-Riñihue (*ca*. 300 Ma; Campos *et al*., 1998) and/or Nahuelbuta (*ca*. 320 Ma; Hervé *et al*., 1976). Alternatively or as a complementary source, they could have been shed from distal Carboniferous granodioritic to leucogranitic rocks of the North-Patagonian Massif (*ca.* 280-300 Ma, U-Pb in zircons; Varela *et al*., 2005).

Zircons of uppermost Devonian-Carboniferous age (360 Ma) could have derived from Devonian granites locally present in the subsurface of the Central Depression (*e.g*., 359.3±4.4 Ma, $^{40}Ar/^{39}Ar$ in amphibole; Duhart *et al*., 1998[1]).

A possible proximal source for Devonian zircons (388, 390 and 412 Ma) is the Chaitén Metatonalite from the western part of the North Patagonian Cordillera (400±5 Ma, U-Pb in zircon; SERNAGEOMIN-BRGM, 1995[2]). Possible distal sources of deposition are the Devonian tonalites and leucogranitic intrusions exposed at the eastern side of the North-Patagonian Cordillera (*ca*. 386-419 Ma, U-Pb in zircons; Varela *et al*., 2005) and the El Laurel Tonalite from the Deseado Massif in the argentinean hinterland (395±4 Ma, U-Pb SHRIMP in zircons; Pankhurst *et al*., 2003).

A possible source for Ordovician zircons (462 and 465 Ma) could be the Dos Hermanos Granite from the Deseado Massif (≥465 Ma, U-Pb SHRIMP in zircons; Pankhurst *et al*., 2003).

Mesoproterozoic detrital zircons have been reported for the Eastern Andean Metamorphic Complex further south in Aisén (Hervé *et al*., 2003b). The authors concluded that these grains probably were derived from cratonic areas within the interior of Gondwana (Hervé *et al*., 2003b).

Assuming that the rocks of the BMMC in the study area cooled monotonously following greenschist facies metamorphism, a linear correlation between K-Ar and $^{40}Ar/^{39}Ar$ and zircon FT cooling ages suggests very slow cooling rates between ~240 Ma and 140 Ma. The wide time-span allows the possibility of previous exhumation of the BMMC followed by reburial before the onset of cooling beneath the ZPAZ in Late Jurassic to Early Cretaceous times. In the Valdivia area, exhumation of the BMMC was reported to have occurred earlier (*e.g.,* Glodny *et al*., 2005). This is supported by zircon FT ages indicating cooling below the ZPAZ by 186±24 Ma (Glodny *et al*., 2005). The oldest zircon FT sample from the basement rocks in the NSIC (AA14, Fig. 6) yielded a Late Jurassic FT central age (156±10 Ma) with moderate age dispersion (11%) and the modeling of its FT single grain-age distribution yielded two populations. Its oldest deconvoluted peak of 198 Ma (C.I. +29/-25 Ma; 32.9%) overlaps with the zircon FT data by Glodny *et al.* (2005). The younger component is late Early Cretaceous (141 Ma; C.I. +13/12 Ma; 67.1%), and could be related to a later episode of exhumation after reburial, a younger thermal resetting event by magmatism at depths within or below the ZPAZ, to differential annealing properties of individual zircon grains by alpha radiation damage or variations of the internal properties of the grains within the sample, or finally due to a combination of these geological processes and internal factors. For the same sample, its apatite FT central age of 67±11 Ma indicates cooling below the APAZ in the Late Cretaceous, although due to its high dispersion (43%), this central age may not necessarily represent exhumation as the fission tracks in the apatites could be partially annealed by later shallow magmatism (Fig. 7).

It should be noted that to the north of the studied area, at the 40ºS, outcrops of Upper Triassic continental clastic units (*e.g.,* Tralcán and

[2] SERNAGEOMIN-BRGM, 1995. Carta Metalogénica de la X Región Sur, Chile. Informe Registrado IR-95-05 (Unpublished), Servicio Nacional de Geología y Minería-Bureau de Recherches Géologiques et Minières, 4 Tomos, 10 Vols., 95 p.

Panguipulli formations) evidence an important contribution of sediments shed by erosion of the BMMC (Martin *et al*., 1999), whereas at the 35ºS in the Coastal Ranges, Triassic-Jurassic volcano-sedimentary sequences overlying metamorphic basement rocks display mineralogical assemblages indicative of very low-grade metamorphic conditions (Belmar and Morata, 2005). Assuming monotonous cooling since the Middle Triassic, this implies that northwards of the CSIC, part of the complex had already emerged to the surface while the basement rocks of the Chiloé Archipelago were at depths close to peak conditions of greenschist facies metamorphism. Triassic rocks have not been found in the Chiloé Archipelago, although previous mapping campaigns have identified metasedimentary rocks of possible Triassic age intruded by the North Patagonian Batholith in the Principal Cordillera (SERNAGEOMIN-BRGM, 1995[2]).

The Late Cretaceous zircon and apatite FT ages from the CSIC are more intriguing. Based on two FT samples taken from nearby Castro and regional contact relationships of the basement rocks with the North Patagonian Batholith, Thomson and Hervé (2002) reported two Late Jurassic zircon FT ages with discordant single-grain age distributions and one Late Cretaceous apatite FT age with small age dispersion. These were interpreted as an effect of thermal overprinting by unidentified parts of the batholith emplaced near the subsurface. The inferred Cretaceous cooling episode however predates the intrusion age of the Metalqui Pluton on the same segment of the Main Chiloé Island (see Figs. 2 and 4).

Alternatively, the cooling of the basement rocks can be related to an episode of uplift and erosion in the Late Cretaceous. This is supported by seismic and borehole data indicating that the forearc basin at the western slope of the Main Chiloé Island has a thickness of ~4 km (González, 1989; Fig. 3). The forearc basin rocks were loosely assigned to the Mesozoic based on regional stratigraphic correlations with other basins found along the coast of southern Chile (González, 1989). Early Cretaceous (Barremian to Aptian) palynomorphs have been described in sedimentological logs from a comparably deep forearc basin at Taitao Peninsula (Puerto Barroso Formation; Diemer *et al.*, 1997).

Within the Main Chiloé Island our reported zircon and apatite FT central ages range from Late Jurassic (*ca*. 156 Ma) to Eocene (*ca.* 38 Ma) and are accompanied by relatively large age dispersions (Table 2, Fig. 4). The modelling of the zircon FT single-grain age distributions for samples within these areas (Table 3, Fig. 6) depicted younger deconvoluted Late Cretaceous peak (*ca*. 80 Ma) postdating Jurassic to Early Cretaceous populations. The modelling of the apatite FT single-grain age distributions from the same area showed two significant populations (Table 4, Fig. 7), an older Late Cretaceous peak (*ca*. 64-91 Ma) and a younger Eocene peak (*ca.* 38-53 Ma), which we interpret as related to a shallow magmatic event that partially reset the grains when they were near the surface. The reproducibility of the modeled ages is hampered due to the few available grains in the samples and the low-U concentration of the apatites, which imply larger intervals of confidence for the modeled peaks. However, one previously dated apatite sample with sufficient FT-length measurements reported for the basement rocks near Castro by Thomson and Hervé (2002) indicated rapid monotonous cooling by 67.5±7.5 Ma. Altogether these data suggest that an important contribution of sediments at the forearc occurred during the Late Cretaceous.

Both, the apatite central FT ages and the younger deconvoluted peaks from the CSIC are as young as Eocene, these probably represent thermal resetting by shallow magmatism, coeval with the Gamboa Dacite and possibly the Metalqui Pluton.

The early to 'mid-Cenozoic' magmatic activity correlates well with an episode of widespread extension that resulted in the subsidence of the Central Depression (*e.g*., Muñoz *et al.*, 2000). During a time-span of 30 my, approximately 3 km of terrigenous and volcaniclastic rocks were deposited. The arrival and subduction of the active-spreading Chile Ridge beneath the Taitao Peninsula by ~10 to 6 Ma triggered a generalized episode of right-lateral transpression, differential block uplift, enhanced cooling and denudation of the arc region along the Liquiñe-Ofqui Fault Zone (*e.g*., Cembrano *et al*., 2000; Thomson *et al*., 2001; Adriasola *et al*., 2006). This was succeeded by ~1 km Pliocene-Pleistocene glacial and volcaniclastic deposits in the Central Depression (Fig. 3), which reflect increased sedimentation rates following erosion of the arc (Adriasola *et al*., 2006).

More recent episodes of differential uplift and erosion along the segments of the Main Chiloé Island were not registered by fission track thermochronology in the studied region. However, this does not preclude further tectonic activity in

the forearc, it only means that during denudation the 100°C isotherm in the forearc did not reach the surface.

5. Conclusions

The youngest dated concordant detrital fraction zircons from the BMMC of the Main Chiloé Island (Duhart *et al*., 1999; Duhart *et al*., 2001; this work) indicate Devonian for the Northern Segment (NSIC) and Late Carboniferous for the Central Segment (CSIC) maximum sedimentation ages. In addition, they suggest a Devonian and Carboniferous sediment sources for at least one part of the BMMC protolith in the Main Chiloé Island. These maximum sedimentation ages are older than the Late Triassic and Permian sedimentation ages defined for the Chonos Metamorphic Complex (Fang *et al*., 1998; Hervé *et al*., 2003a) and Metasedimentary Duque de York Complex (Hervé *et al*., 2003a; Lacassie *et al*., 2006) respectively, and are in agreement with previously reported maximum sedimentation ages for the BMMC (Duhart *et al*., 2001) and the Main Range Metamorphic Complex (Hervé *et al*., 2003a), and are partially overlapping with the Devonian-Late Triassic maximum sedimentation age defined for the Eastern Andean Metamorphic Complex (Hervé *et al*., 2003a; Augustsson *et al*., 2006). Other older concordant detrital zircon fraction indicate Ordovician and Mesoproterozoic (Grenvillian) primary source ages.

The K-Ar and $^{40}Ar/^{39}Ar$ ages ranging between 245 and 220 Ma represent the cooling ages related to the Ar closure temperature in muscovite near to 350°C, and they are temporally close to the maximum temperature of greenschist facies metamorphism. Thus, the greenschist facies metamorphism would have happened during the Early to Middle Triassic times. The available K-Ar and $^{40}Ar/^{39}Ar$ ages for the metamorphic rocks in Chiloé Archipelago show partial correlation to the cooling ages reported for the BMMC further the north of the study area.

The stratigraphic position of the basement rocks, underlying Upper Triassic continental sedimentary rocks, is in agreement with the cooling and maximum sedimentation ages obtained in this research work.

On main Chiloé Island, 5 zircon and 7 apatite FT ages were obtained in rocks of the BMMC. These range between Late Jurassic and Early Eocene. The zircon FT central ages of the metamorphic basement from the CSIC and SCIC indicate the onset of cooling below ~220-350°C since the early Late Cretaceous. This is interpreted as cooling following exhumation of the complex from depths of *ca.* 10-12 km at this time, and is supported by the presence of a ~4 km thick sedimentary basin of presumably Mesozoic age (Paleogene and older) at the western slope of the forearc bounding the emerged complex along steep-dipping inverted basement faults.

The modelling of the apatite FT single-grain age distributions indicates Late Cretaceous and Eocene peaks. The older deconvoluted apatite FT ages from samples of the CSIC are inferred to relate to exhumation of the basement rocks in the early Late Cretaceous. The younger modelled apatite FT age populations suggest thermal resetting by the presence of shallow-level intrusions within this segment. The late cooling episode is probably closely related to the Early Eocene intrusion of the recently discovered Metalqui Pluton and to the shallow intrusions such as Gamboa Dacite.

The presence of inverted Cenozoic faults along the western margin of the main Chiloé Island with exposed Miocene marine terraces facing the Pacific coast, indicate that differential uplift and denudation has continued in the forearc region since the Late Eocene.

Acknowledgements

The authors thank J. Muñoz, F. Hervé and C. Mpodozis for their valuable suggestions, observations and motivation in writing this manuscript. This contribution benefited greatly from very constructive reviews by S.N. Thomson, H. Miller and F. Hervé.

This work forms part of the project 'Estudio Geológico y Geoambiental de Chiloé Insular y del sector Occidental de la IX Región', by the Puerto Varas Technical Office of the Servicio Nacional de Geología y Minería (Sernageomin). U-Pb chronology was carried out in the Massachusetts Institute of Technology (USA) by M. Martin. A.C.A. was sponsored by DAAD Grant A/99/02931. Early field work was funded by DFG Grant Sto 196/11-2 and by Fondecyt Grant 1980741 to F. Hervé from the Universidad de Chile.

References

Adriasola, A.C. 2003. Low Temperature Thermal History and Denudation along the Liquiñe-Ofqui Fault Zone in the Southern Chilean Andes, 41-42°S. Rühr-Universität Bochum, Ph.D. Thesis (Unpublished): 119 p. urn:nbn:de:hbz:294-11509. Bochum, Germany.

Adriasola A.C.; Thomson, S.N.; Brix, M.R.; Hervé, F.; Stöckhert, B. 2006. Postmagmatic cooling and late Cenozoic denudation of the North Patagonian Batholith in the Los Lagos region of Chile, 41°-42°15' S. International Journal of Earth Sciences 95 (3): 504-528.

Aguirre, L.; Hervé, F.; Godoy, E. 1972. Distribution of metamorphic facies in Chile-An outline. Krystalinikum 9: 7-19.

Antinao, J.L.; Duhart, P.; Clayton, J.; Elgueta, S.; McDonough, M. 2000. Área de Ancud-Maullín. Servicio Nacional de Geología y Minería, Mapas Geológicos, No. 17, 1 mapa escala 1:100.000. Santiago.

Arenas, M.; Duhart, P. 2003. Geología del Área Castro-Dalcahue. Servicio Nacional de Geología y Minería, Carta Geológica de Chile, Serie Geología Básica 79: 31 p., 1 mapa escala 1:100.000. Santiago.

Augustsson, C.; Münker, C.; Bahlburg, H.; Fanning M. 2006. Provenance of late Palaeozoic metasediments of the SW South American Gondwana margin: a combined U-Pb and Hf-isotope study of single detrital zircons. Journal of the Geological Society of London 163: 983-995.

Bangs, N.; Cande, S. 1997. Episodic development of a convergent margin inferred from structures and processes along the southern Chile margin. Tectonics 16 (3): 489-503.

Beck M.E.; Rojas, C.; Cembrano, J. 1993. On the nature of buttressing in margin-parallel strike-slip fault systems. Geology 21: 755-758.

Belmar, M.; Morata, D. 2005. Nature and P-T-t constraints of very low grade metamorphism in the Triassic-Jurassic basins, Coastal Range, central Chile. Revista Geológica de Chile 32 (2): 189-205.

Brandon, M.T. 1996. Probability-density plots for fission-track grain-age distributions. American Journal of Science 292: 535-564.

Brandon, M.T. 2002. Decomposition of mixed grain age distributions using Binomfit. On Track 24: 13-18.

Brandon, M.T.; Roden-Tice, M.K.; Garver, J. 1998. Late Cenozoic exhumation of the Cascadia accretionary wedge in the Olympic Mountains, northwest Washington State. Geological Society of America Bulletin 110: 985-1009.

Campos, A.; Moreno, H.; Muñoz, J.; Antinao, J.; Clayton, J.; Martin, M. 1998. Área de Futrono-Lago Ranco. Servicio Nacional de Geología y Minería, Mapas Geológicos 8, 1 mapa escala 1:100.000. Santiago.

Cembrano, J.; Schermer, E.; Lavenu, A.; Sanhueza, A. 2000. Contrasting nature of deformation along an intra-arc shear zone, The Liquiñe-Ofqui Fault Zone, Southern Chilean Andes. Tectonophysics 319: 129-149.

Crignola, P.; Duhart, P.; McDonough, M.; Muñoz, J. 1997. Antecedentes geoquímicos acerca del origen de los esquistos máficos y cuerpos ultramáficos en la Cordillera de la Costa, sector norte de la X^{a} Región, Chile. *In* Congreso Geológico Chileno, No. 8, Actas 2: 1254-1258. Antofagasta.

Dewey, J.F.; Lamb, S.H. 1992. Active tectonics of the Andes. Tectonophysics 205: 79-95.

Díaz, L.; Vivallo, W.; Alfaro, G.; Cisternas, M. 1988. Geoquímica de los Esquistos Paleozoicos de Bahía Mansa, Osorno, Chile. *In* Congreso Geológico Chileno, No. 5, Actas 2: E75-E96. Santiago.

Diemer, J.A.; Forsythe, R.D.; Engelhardt, D.; Porter, C. 1997. An Early Cretaceous forearc basin in the Golfo de Penas region, southern Chile. Journal of the Geological Society of London 154 (6): 925-928.

Duhart, P.; Muñoz, J.; McDonough, M.; Martin, M.; Villeneuve, M. 1999. $^{207}Pb/^{206}Pb$ and $^{40}Ar/^{39}Ar$ Geochronology of the Coastal Metamorphic Belt between 41-42º S in central-south Chile. *In* International Symposium on Andean Geodynamics, No. 4, Actas 1: 219-223. Göttingen.

Duhart, P.; Muñoz, J.; Stern, C. 2000. Geología de la Isla Grande de Chiloé, X Región de Los Lagos, Chile. *In* Congreso Geológico Chileno, No. 9, Actas 1: 461-465. Puerto Varas.

Duhart, P.; McDonough, M.; Muñoz, J.; Martin, M.; Villeneuve, M. 2001. El Complejo Metamórfico Bahía Mansa en la Cordillera de la Costa del centro-sur de Chile (39°30'-42°00' S): geocronología K-Ar, $^{40}Ar/^{39}Ar$ y U-Pb e implicancias en la evolución del margen sur-occidental de Gondwana. Revista Geológica de Chile 28 (2): 179-208.

Duhart, P.; Muñoz, J. 2001. K-Ar geochronologic evidence for a Triassic metamorphic event in the Main Chiloé Island, south-central Chile. *In* Simposio Sudamericano de Geología Isotópica, No. 3, Actas: 566-569. Pucón.

Elgueta, S.; McDonough, M.; LeRoux, J.; Urqueta, E.; Duhart, P. 2000. Estratigrafía y Sedimentología de las Cuencas Terciarias, Región de Los Lagos (39-42º S), Chile. Servicio Nacional de Geología y Minería, Boletín 57: 52 p.

Fang, Z.J.; Boucot, A.; Covacevich, V.; Hervé, F. 1998. Discovery of Late Triassic fossils in the Chonos Metamorphic Complex, southern Chile. Revista Geológica de Chile 25 (2): 165-173.

Fortey, R.; Pankhurst, R.J.; Hervé, F. 1992. Devonian Trilobites at Buill, Chile (42°S). Revista Geológica de Chile 19 (2): 133-144.

Galbraith, R.F. 1990. The radial plot: graphical assessment of spread in ages. Nuclear Tracks 17: 207-214.

Galbraith, R.F.; Green, P.F. 1990. Estimating the component ages in a finite mixture. Nuclear Tracks 17: 197-206.

Galbraith R.F.; Laslett G.M. 1993. Statistical models for mixed fission track ages. Nuclear Tracks 21: 459-470.

Glodny, J.; Lhormann, J.; Echtler, H.; Gräfe, K.; Seifert, W.; Collao, S.; Figueroa, O. 2005. Internal dynamics of a paleoaccretionary wedge: insights from combined

isotope tectonochronology and sandbox modelling of the South-Central Chilean forearc. Earth and Planetary Sciences Letters 231: 23-39.

González, E. 1989. Hydrocarbon resources in the coastal zone of Chile. *In* Geology of the Andes and its relation to hydrocarbon and mineral resources (Ericksen, G.E.; Cañas M.T.; Reinemund, J.A.; editors). Circum-Pacific Council for Energy and Mineral Resources Earth Science Series, 11: 383-404.

Godoy, E.; Kato, T. 1990. Late Paleozoic serpentinites and mafic schists from the Coast Range accretionary complex, central Chile: their relation to aeromagnetic anomalies. Geologische Rundschau 70: 121-130.

Gradstein, F.; Ogg, J.; Smith, A.; Bleeker, W.; Lourens, L. 2004. A new Geologic Time Scale with special reference to Precambrian and Neogene. Episodes 27 (2): 83-100.

Green, P.F.; Duddy, I.R.; Laslett, G.M.; Hegarthy, K.A.; Gleadow, A.J.W.; Lovering, J.F.; 1989. Thermal annealing of fission tracks in apatite: 4. Quantitative modelling techniques and extension to geological time scale. Chemical Geology 79: 155-182.

Hervé, F.; Fanning, M.; Pankhurst, R.J. 2003a. Detrital zircon age patterns and provenance of the metamorphic complexes of southern Chile. Journal of South American Earth Sciences 16: 107-123.

Hervé, F.; Fanning, M.; Thomson, S.N.; Pankhurst, R.J.; Anma, R.; Veloso, A.; Herrera, C. 2003b. SHRIMP U-Pb and FT Pliocene ages of near-trench granites in Taitao Peninsula, southern Chile. *In* Simposium Sudamericano de Geología Isotópica, No. 4, Actas: 190-193. Salvador.

Hervé, F.; Munizaga, F.; Mantovani, M.; Hervé, M. 1976. Edades Rb-Sr Neopaleozoicas del Basamento Cristalino de la Cordillera de Nahuelbuta. *In* Congreso Geológico Chileno, No. 1, Actas 1: F19-F26. Santiago.

Heusser, C.J. 1990. Chilotan Piedmont Glacier in the Southern Andes during the glacial maximum. Revista Geológica de Chile 17 (1): 3-18.

Hufmann, L. 2003. Thermobarometrische und geochemische Untersuchungen der Gesteine der Küstenkordillere Chiloés, Südchile. Von der Fakültat Bio-und Geowissenschaften der Universität Stuttgart zur Erlangung der Würde einer Doktorin del Naturwissenschaften genehmigte Abhandlung: 240 p. Stuttgart.

Hufmann, L.; Massonne, H. 2000. Ancient arc/back-arc and N-MORB volcanics incorporated in the Late Palaeozoic/Early Mesozoic metamorphic complex of the Coastal Cordillera of Chiloé, Southern Central Chile. *In* Congreso Geológico Chileno, No. 9, Actas 2: 738-741. Puerto Varas.

Hurford, A.J.; Green, P.F. 1983. The zeta age calibration of fission track dating. Chemical Geology 1: 285-317.

Hurford, A.J.; Hunziker, J.C.; Stöckhert, B. 1991. Constraints on the thermotectonic evolution of the Western Alps: evidence for episodic rapid uplift. Tectonics 10: 758-769.

Hurford, A.J. 1990. Standardization of fission track dating calibration: recommendation by the Fission Track Working Group of the I.U.G.S. Subcommission on Geochronology. Chemical Geology 80: 171-178.

Jaffey, A.H.; Flyn, K.F.; Glendenin, L.E.; Bentley, W.C.; Essling, A.M. 1971. Precision measurement of half-lives and specific activities of ^{235}U and ^{238}U. Physical Review 4 (5): 1.889-1.906.

Kasuya, M.; Naeser, C.W. 1988. The effect of a-damage on fission-track annealing in zircon. Nuclear Tracks Radiation Measurements (l14): 477-480.

Kato, T. 1985. Pre-Andean orogenesis in the Coast Range of central Chile. Geological Society of America Bulletin 96: 918-924.

Kato, T.; Godoy, E. 1995. Petrogenesis and tectonic significance of Late Paleozoic coarse-crystalline blueschist and amphibolite boulders in the Coastal Range of Chile. International Geology Review 37: 992-1006.

Lacassie, J.P.; Hervé, F.; Roser, B. 2006. Sedimentary provenance study of the post-Early Permian to pre-Early Cretaceous metasedimentary Duque de York Complex, Chile. Revista Geológica de Chile 33 (2): 199-219.

Lagabrielle, I.; Guivel, C.; Maury, R.; Bourgois, J.; Fourcade, S.; Martin, H. 2000. Magmatic-tectonic effects of high thermal regime at the site of active ridge subduction: the Chile Triple Junction model. Tectonophysics 326: 255-268.

Laslett, G.M.; Kendall, W.S.; Gleadow A.J.W.; Duddy, I.R. 1982. Bias in measurement of fission track length distributions. Nuclear Tracks 6: 79-85.

Levi, B.; Aguilar, A.; Fuenzalida, R. 1966. Reconocimiento Geológico en las Provincias de Llanquihue y Chiloé. Instituto de Investigaciones Geológicas, Boletín (19): 45 p.

Ludwig, K.R. 1980. Calculation of uncertainties of U-Pb isotope data. Earth and Planetary Sciences Letters 46: 212-220.

Martin, M.; Kato, T.; Rodríguez, C.; Godoy, E.; Duhart, P.; McDonough, M.; Campos, C. 1999. Evolution of late Paleozoic accretionary complex and overlying forearc-magmatic arc, south-central Chile (38-41°S): Constraints for the tectonic setting along the southwestern margin of Gondwana. Tectonics 18 (4): 582-605.

Martínez, R.; Pino, M. 1979. Edad, paleoecología y sedimentología del Mioceno Marino de la Cuesta de Santo Domingo, Provincia de Valdivia, X Región. *In* Congreso Geológico Chileno, No. 2, Actas, 3: H103-H124. Arica.

McDonough, M.; Ugalde, H.; Duhart, P.; Crignola, P. 1997. Nuevos antecedentes estructurales de la Cordillera de la Costa y el adyacente Valle Central en la parte norte de la X Región, Chile: su relación con el patrón magnético. *In* Congreso Geológico Chileno, No. 8, Actas 1: 36-40. Antofagasta.

Massonne, H.; Hervé, F.; Medenbach, O.; Muñoz, V.;

Willner, A. 1998. Zussmanite in ferrigenous metasediments from Southern-Central Chile. Mineralogical Magazine 62 (6): 869-876.

Massonne, H.; Hervé, F.; Muñoz, V.; Willner, A. 1996. New petrological results on high-pressure, low-temperature metamorphism of the Upper Paleozoic basement of Central Chile. *In* Symposium International Sur la Géodynamique Andine, No. 3, Actas: 783-785. Saint Malo.

Mordojovic, C.; Álvarez, J. 1977. Morfología de la Plataforma Continental de Chile del sector Valdivia-Isla Guafo. Ciencia y Tecnología del Mar, CONA 3: 9-22. Santiago.

Mpodozis, C.; Hervé, M.; Nasi, C.; Soffia, J.M.; Forsythe, R.; Nelson, E. 1985. El magmatismo Plioceno de la Península Tres Montes y su relación con la evolución del Punto Triple de Chile austral. Revista Geológica de Chile (25-26): 13-28.

Munizaga, F.; Hervé, F.; Drake, R.; Pankhurst, R.; Brook, M.; Snelling, N. 1988. Geochronology of the Lake Region of South-Central Chile (39-42º S): Preliminary results. Journal of South American Earth Sciences 1 (3): 309-316.

Mercer, J.H. 1976. Glacial History of Southernmost South America. Quaternary Research 6: 125-166.

Muñoz, J.; Duhart, P.; Hufmann, L.; Massone, H.; Stern C. 1999. Geologic and structural setting of Chiloé Island, Chile. *In* Congreso Geológico Argentino, No. 14, Actas 1: 182-184. Salta.

Muñoz, J.; Troncoso, R.; Duhart, P.; Crignola, P.; Farmer, L.; Stern, C. 2000. The relation of the mid-Tertiary coastal magmatic belt in south-central Chile to the late Oligocene increase in plate convergence rate. Revista Geológica de Chile 27 (2): 177-203.

Naeser, C.W. 1976. Fission track dating. U.S. Geological Survey Open File Report, Vol. 76-190.

Nasdala, L.; Wenzel, M.; Vavra, G.; Wenzel, T.; Bernd, K. 2001. Metamictization of natural zircon: accumulated versus thermal annealing of radioactivity-induced damage. Contributions to Mineralogy and Petrology 142: 125-144.

Pankhurst, R.J.; Weaver, S.D.; Hervé, F.; Larrondo, P. 1999. Mesozoic-Cenozoic evolution of the North Patagonian Batholith in Aysén, southern Chile. Journal of the Geological Society of London 156: 673-694.

Pankhurst, R.J.; Rapela, C.W.; Loske, W.P.; Márquez, M.; Fanning, C.M. 2003. Chronological study of the pre-Permian basement rocks of southern Patagonia. Journal of South American Earth Sciences 16: 27-44.

Porter, S.C. 1981. Late Pleistocene Glaciation in Southern Lake District of Chile. Quaternary Research 16: 263-292.

Quiroz, D.; Duhart, P.; Crignola, P. 2004. Geología del Área Chonchi-Cucao. Servicio Nacional de Geología y Minería, Carta Geológica de Chile, Serie Geología Básica (86): 33 p., 1 mapa escala 1:100.000. Santiago.

Quiroz, D.; Duhart, P.; Muñoz, J. 2006. Antecedentes Geocronológicos del Magmatismo Cretácico Superior y Eoceno de la Cordillera de la Costa del centro-sur de Chile (39-43°S): Implicancias Paleogeográficas. *In* Congreso Geológico Chileno, No. 11, Actas 2: 539-542.

Rahn, M.K.; Brandon, M.T.; Batt, G.E.; Garver, J.I. 2004. A zero model for fission-track annealing in zircon. American Mineralogy 89: 473-484.

Reyners, W.P.; Brandon, M.T. 2006. Using Thermochronology to Understand Orogenic Erosion. Annual Review of Earth and Planetary Sciences (34): 419-466.

Rojas, C.; Beck, M.E.; Burmester, R.F.; Cembrano, J.; Hervé, F. 1994. Paleomagnetism of the mid-Tertiary Ayacara Formation, southern Chile: Counterclockwise rotation in a dextral shear zone. Journal of South American Earth Sciences 7: 45-56.

Saliot, P. 1969. Etude géologique dans l`ile de Chiloé (Chile). Bullettin Sociéte Géologique Francaise 7 (11): 388-399.

Schmitz, M.D.; Bowring, S.A. 2001. U-Pb zircon and titanite systematic of the Fish Canyon Tuff: an assessment of high-precision U-Pb geochronology and its applications to young volcanic rocks. Geochimica et Cosmochimica, Acta 65 (15): 2581-2597.

Stern, C.; Vergara, M. 1992. New age of the vitrophyric rhyolite-dacite from Ancud (42°S), Chiloé, Chile. Revista Geológica de Chile 19 (2): 249-251.

Tagami T.; Shimada, C. 1996. Natural long-term annealing of the zircon fission-track system around a granitic pluton. Journal of Geophysical Research 101: 8245-8255.

Tavera, J.; Valdivia, S.; Valenzuela, E. 1985. Mioceno fosilífero del sur de Chile: Isla de Chiloé a Peninsula de Taitao. *In* Congreso Geológico de Chile, No. 4, Actas 1: 546-568. Antofagasta.

Thomson, S.N. 2002. Late Cenozoic geomorphic and tectonic evolution of the Patagonian Andes between latitudes 42° and 46°S: an appraisal based on fission track results from the transpressional intra-arc Liquiñe-Ofqui Fault Zone. Geological Society of America Bulletin 9 (114): 1159-1173.

Thomson, S.N.; Hervé, F. 2002. New time constraints for the age of metamorphism at the ancestral Pacific Gondwana margin of southern Chile (42°-52°S). Revista Geológica de Chile 29 (2): 255-271.

Thomson, S.N.; Hervé, F.; Stöckhert, B. 2001. The Mesozoic-Cenozoic denudation history of the Patagonian Andes (southern Chile) and its correlation to different subduction processes. Tectonics 20: 693-711.

Valenzuela, E. 1982. Estratigrafía de la boca occidental del Canal de Chacao, Xª Región, Chile. *In* Congreso Geológico Chileno, No. 3, Actas 1: A343-A376. Antofagasta.

Varela, R.; Basei, M.; Cingolani, C.; Siga, O.; Passarelli, C. 2005. El basamento cristalino de los Andes patagónicos

en Argentina: geocronología e interpretación tectónica. Revista Geológica de Chile 32 (2): 167-187.

Vergara, M.; Munizaga, F. 1974. Age and Evolution of the Upper Cenozoic Volcanism in Central-south Chile. Geological Society of America Bulletin 85: 603-606.

Watters, W.A.; Fleming, F.R.S. 1972. Contribution to the Geology and Palaeontology of Chiloé Island, Southern Chile. Philosophical Transactions of the Royal Society of London 263 (853): 369-408.

Willner, A.P.; Glodny, J.; Gerya, T.V.; Godoy, E.; Massonne, H. 2004. A counterclockwise *PTt* path of high-pressure/low-temperature rocks from the Coastal Cordillera accretionary complex of south-central Chile: constraints for the earliest stage of subduction mass flow. Lithos 75: 283-310.

Manuscript received: September 26, 2006; accepted: May 08, 2007.